

1 **Draft genome of the honey bee ectoparasitic mite, *Tropilaelaps mercedesae*, is shaped by the**
2 **parasitic life history**

33
44
55
65 Xiaofeng Dong¹, Stuart D Armstrong², Dong Xia², Benjamin L. Makepeace², Alistair C. Darby³, and
76 Tatsuhiko Kadowaki^{1*}

87
108
119 ¹Department of Biological Sciences, Xi'an Jiaotong-Liverpool University, 111 Ren'ai Road, Suzhou
120 Dushu Lake Higher Education Town, Jiangsu Province 215123, China

141 ²Institute of Infection & Global Health, University of Liverpool, Liverpool L3 5RF, United Kingdom

162 ³Institute of Integrative Biology, University of Liverpool, Liverpool L69 7ZB, United Kingdom

173
184
194 Corresponding author:

205 Tatsuhiko Kadowaki

216 Department of Biological Sciences, Xi'an Jiaotong-Liverpool University

217 111 Ren'ai Road, Suzhou Dushu Lake Higher Education Town

248 Jiangsu Province 215123, China

269 TEL: 86 512 88161659, FAX: 86 512 88161899

270 E-mail: Tatsuhiko.Kadowaki@xjtlu.edu.cn

302 E-mail addresses of authors:

313 Xiaofeng Dong: Xiaofeng.dong12@student.xjtlu.edu.cn

324 Stuart D Armstrong: sarmstro@liverpool.ac.uk

345 Dong Xia: dongxia@liverpool.ac.uk

326 Benjamin L. Makepeace: blm1@liverpool.ac.uk

377 Alistair C. Darby: Alistair.Darby@liverpool.ac.uk

31 **Abstract**

32 **Background**

33 The number of managed honey bee colonies has considerably decreased in many developed
34 countries in recent years and ectoparasitic mites are considered as major threats to honey bee
35 colonies and health. However, their general biology remains poorly understood.

36 **Results**

37 We sequenced the genome of *Tropilaelaps mercedesae*, the prevalent ectoparasitic mite infesting
38 honey bees in Asia and predicted 15,190 protein-coding genes which were well supported by the
39 mite transcriptomes and proteomic data. Although amino acid substitutions have been accelerated
40 within the conserved core genes of two mites, *T. mercedesae* and *Metaseiulus occidentalis*, *T.*
41 *mercedesae* has undergone the least gene family expansion and contraction between the seven
42 arthropods we tested. The number of sensory system genes has been dramatically reduced but *T.*
43 *mercedesae* contains all gene sets required to detoxify xenobiotics. *T. mercedesae* is closely
44 associated with a symbiotic bacterium (*Rickettsiella grylli*-like) and DWV, the most prevalent honey
45 bee virus.

46 **Conclusions**

47 *T. mercedesae* has a very specialized life history and habitat as the ectoparasitic mite strictly depends
48 on the honey bee inside a stable colony. Thus, comparison of the genome and transcriptome
49 sequences with those of a tick and free-living mites has revealed the specific features of the genome
50 shaped by interaction with the honey bee and colony environment. Genome and transcriptome
51 sequences of *T. mercedesae*, as well as *Varroa destructor* (another globally prevalent ectoparasitic
52 mite of honey bee), not only provide insights into the mite biology, but may also help to develop
53 measures to control the most serious pests of the honey bee.

54
55 **Keywords:** Honey bee decline, Honey bee ectoparasitic mite, Genome, Transcriptome, Proteome,
56 Comparative genomics, Host-Parasite interaction

Background

The number of managed honey bee (*Apis mellifera*) colonies has considerably decreased in many developed countries in recent years [1]. Although there are many potential causes for the decline, pathogens and parasites of the honey bee, particularly ectoparasitic mites, are considered major threats to honey bee colonies and health [2]. *Varroa destructor* is present globally and causes abnormal brood development and brood death in honey bees, and is also responsible for the spread of honey bee pathogens and parasites [3]. *Tropilaelaps mercedesae* (small honey bee mite, Fig. 1) is another honey bee ectoparasitic mite which is prevalent in most Asian countries [4]. Thus, these two mite species usually co-exist in a honey bee colony in Asia. Compared to *V. destructor*, *T. mercedesae* produces a higher number of offspring and has almost no phoretic period on adult honey bees, and thus builds up relatively higher population levels within colonies [4, 5]. Similar to *V. destructor*, *T. mercedesae* can vector Deformed Wing Virus (DWV) [6, 7] and influence host immune responses [8]. Furthermore, it has been recently shown that *T. mercedesae* infestation reduces the longevity and emergence weight of honey bees, and enhances the DWV levels and associated symptoms [9]. The original host of *T. mercedesae* is the giant Asian honey bee, *Apis dorsata*, and like *V. destructor*, it shifted hosts to infest *A. mellifera* when these colonies were brought into Asia [4]. Although *T. mercedesae* is currently restricted to Asia, it has the potential to spread and establish all over the world due to the global trade of honey bees. This is exactly what happened with *V. destructor* [10].

T. mercedesae and *V. destructor* are major threats to the current apiculture industry; however, we still do not completely understand their sensory system, development, sex determination/differentiation, reproduction, and the capability to acquire miticide (for example, tau-fluvalinate and flumethrin) resistance. Genomic features of *V. destructor* were briefly reported before and the associated bacteria and viruses were identified [11]. In this study, we sequenced the genome and transcriptomes of *T. mercedesae*, supplemented by proteomic data, to provide insights into the above aspects and understand how the mite has evolved under a very specialized environment - inside the honey bee colony by depending on the honey bee as the sole host. We will discuss how *T. mercedesae* may have adapted to its host and environment by shaping its genome.

Results and Discussion

Genome assembly, repeated sequences, and gene annotation

Dual indexed paired-end DNA libraries were prepared from a single adult male and female *T. mercedesae* for whole-genome sequencing using the Illumina shotgun platform (Supplementary Table 1). The “cleaned” reads from the male mite were then re-assembled into 34,155 scaffolds with an N50 of 28,807 bp representing ~353 Mb of genomic sequence, from which we predicted 15,190 protein-coding genes (Table 1 and Supplementary Table 2). We found that 95.33% of the “cleaned reads” could be mapped back to this assembly and 244 (98.4%) out of the 248 Conserved Eukaryotic Genes [12] as well as 83% of 2,675 arthropod BUSCOs [13] were annotated from the assembled genome (Supplementary Table 3). These are comparable to those reported for nine other arachnids (Table 1 and Supplementary Table 3). Proteomic characterization of the adult males and females yielded 124,798 mass spectra in total and 60,463 were assigned to the peptides of annotated proteins above (Supplementary file 1). With k-mer statistics [14], the size of the *T. mercedesae* genome was

100 estimated to be 660 Mb with a peak k-mer depth of ~60X, and thus approximately 50% of the
101 genome DNA was inferred to comprise repetitive sequences (Supplementary Fig. 1). Repetitive
102 sequences such as DNA transposons, retrotransposons including LINE (Long Interspersed Nuclear
103 Element), SINE (Short Interspersed Nuclear Element), and LTR (Long Terminal Repeat) as well as
104 satellite DNA represent only 7 % of the assembly. But they occupied 48.57% of total clean reads
105 (Supplementary Table 4) and the majority of them were found in the high-coverage regions of the
106 genome (Supplementary Table 5), suggesting that repetitive sequences have been collapsed in the
107 genome assembly. We thus concluded that the qualities of draft genome sequence and protein-coding
108 gene set were sufficiently robust for further characterization of *T. mercedesae* genome and
109 transcriptome.

110 Flow cytometric measurement of *T. mercedesae* nuclear DNA content together with the k-mer
111 statistics demonstrated that the male mite assumed to be haploid with ~660 Mb (1C) DNA. The
112 female mite was twice that size and assumed to be diploid at 1,287 Mb (2C) DNA (Supplementary
113 Fig. 2). Thus, *T. mercedesae* may use haplodiploidy for sex determination, and the genome size of *T.*
114 *mercedesae* is the largest among those of mites whose genomes have been sequenced (*V. destructor*,
115 *Metaseiulus occidentalis*, *Tetranychus urticae*, *Sarcoptes scabiei*, and *Dermatophagoides farinae*)
116 [15-17, 11, 18] but smaller than those of ticks (for example, *Ixodes scapularis* [19]). As expected
117 from the largest genome size among the sequenced mites, gene density is low in the *T. mercedesae*
118 genome (with larger intergenic regions); reminiscent of the large velvet spider (*Stegodyphus*
119 *mimosarum*) and the black-legged tick (*I. scapularis*) genomes (Supplementary Fig. 3). Although the
120 exon size range was comparable in all tested genomes (small honey bee mite, predatory mite,
121 black-legged tick, velvet spider, spider mite, fruit fly, and honey bee) (Supplementary Fig. 4A), the
122 average size of introns in *T. mercedesae* is larger than that in two other mites and insects that were
123 analyzed (Supplementary Fig. 4B). We also successfully annotated genes encoding rRNA, tRNA,
124 snRNA, and miRNA in the *T. mercedesae* genome (Supplementary Table 6), obtained RNA-seq data
125 from *T. mercedesae* adult males and females as well as nymphs, and assembled the reads to aid
126 protein-coding gene annotation and to compare their gene expression profiles.

127 **Comparative genomics**

128 The protein-coding genes of *T. mercedesae* were compared with those of six other arthropods
129 (mentioned above) and a nematode. Phylogenetic trees constructed using 926 highly conserved 1:1
130 orthologs implementing both maximum likelihood and Bayesian methods demonstrated that the
131 *Tropilaelaps* mite and the predatory mite cluster together; however, the spider mite forms an
132 outgroup to two other mites, the black-legged tick, and the velvet spider (Fig. 2A). This is consistent
133 with previous reports that the subclass Acari is diphyletic, with the superorders Acariformes (spider
134 mite) and Parasitiformes (*Tropilaelaps* mite and predatory mite) being distantly related [20, 21].
135 Since above three mite species have similar body structure and morphology, this could be an
136 example of convergent evolution [22]. The molecular species phylogenetic tree also indicates the
137 variable evolutionary rates in gene sequence; with the branch of *T. mercedesae* and *M. occidentalis*
138 exhibiting the fastest rate among arthropods we tested (Fig. 2A).

139 OrthoMCL classified the predicted proteins of *T. mercedesae* together with proteins from six
140 other arthropods and outgroup into a total of 15,506 orthology clusters. As expected from the
141 phylogenetic tree, the *Tropilaelaps* mite shares the most orthology clusters (1,215) with the

142 predatory mite (Fig. 2B). Among these orthology clusters, GO terms related with 'Structural
143 constituent of cuticle', 'Regulation of DNA methylation', and 'Xenobiotic metabolic process' are
144 enriched (Supplementary Table 7). We found 119 orthology clusters consisting of 332
145 species-specific genes and 5,846 unclustered genes which were not classified to any orthology
146 clusters by orthoMCL are only present in *T. mercedesae* but not in the other reference genomes
147 analyzed (Fig. 2A and B). These unclustered genes may include both *T. mercedesae*-unique genes
148 and paralogs which have extensively diverged from their orthologs so that their sequence similarity
149 was not detected by orthoMCL. We found that 1,981 unclustered genes could be assigned with at
150 least one GO term and among these lineage-specific genes, three GO terms, 'Structural constituent of
151 cuticle', 'Nucleosome', and 'DNA bending complex' are highly enriched ($FDR < 1.50 \times 10^{-4}$)
152 (Supplementary Table 8). *T. mercedesae* contains 117 members of the cuticle protein family [23], in
153 which 53 are novel among the seven arthropods analyzed, suggesting that the mite's exoskeleton has
154 rapidly evolved. Two other enriched GO terms could be involved in the epigenetic control of gene
155 expression. Among 226 orthology clusters that are shared between *T. mercedesae*, *M. occidentalis*,
156 and *I. scapularis*, GO terms related with 'Transporter activity' are highly enriched. We found that 135
157 orthology clusters specifically shared between *T. mercedesae* and *I. scapularis* were enriched with
158 GO terms related to 'Renal tubule development', perhaps to maintain a constant water level following
159 the intake of a large volume of hemolymph or blood, respectively [24, 25] (Supplementary Table 9).

160 We used CAFE to infer gene family expansion and contraction in *T. mercedesae* together with
161 six other arthropod species. We found that *T. mercedesae* has undergone the fewest gene family
162 expansion/contraction events since divergence from the common ancestor of arthropods
163 (Supplementary Fig. 5). This feature may fit to the specific life history of a mite parasitizing only the
164 honey bee and living inside a colony with an enclosed, stable environment. However, there are some
165 significantly expanded gene families (P -value < 0.001) associated with zinc ion binding and peptide
166 cross-linking. Meanwhile, one of the HSP70 gene families (Heat shock 70 kDa protein cognate 4)
167 has significantly contracted in *T. mercedesae* (Supplementary Table 10), perhaps because the mite
168 spends most of its time in the honey bee brood cell where the temperature is constantly around 35°C
169 [26]. We analyzed 91 genes with $d_N/d_S > 1.0$ in *T. mercedesae* using the one ratio model (null model)
170 to test the significance, and found that four genes have evolved rapidly either due to relaxation or
171 positive selection (Supplementary Table 11). Among them, Tm_07523 encodes an
172 endo- β -N-acetylglucosaminidase-like protein, a chitinase, which could be involved in processing
173 chitin specifically present in *T. mercedesae*.

174 Sensory systems

175 *T. mercedesae* has a very specific life history and habitat as a honey bee ectoparasitic mite. The mite
176 depends only on the honey bee as the host and spends most of its life in the capped brood cell. Thus,
177 they are likely to depend on the chemosensory rather than the visual system to seek out the fifth
178 instar honey bee larva and the mating pair. Therefore, we annotated and analyzed genes associated
179 with phototransduction and chemosensory systems in *T. mercedesae*.

180 We found that the homologs of *D. melanogaster* opsins, arrestin, TRPL, and INAD are absent in
181 *T. mercedesae* (Supplementary Fig. 6). Since they are the major components for fruit fly
182 photoreception, *T. mercedesae* appears to be blind, and this is consistent with the lack of eye
183 structures. Nevertheless, the adult females immediately move out from a brood cell when the cap is

184 removed and exposed to light, suggesting that they may be able to respond to light. *T. mercedesae*
185 has two *peropsin* genes, as do predatory mites [21] (Supplementary Fig. 7). Peropsin is a retinal
186 photoisomerase that converts all-*trans*-retinal to 11-*cis*-retinal and may couple with a G-protein
187 through the conserved 'NPXXY' motif at the seventh transmembrane domain [27]. The existence of
188 this gene in the jumping spider, black-legged tick, and humans suggests that peropsin may have been
189 lost specifically in insects. However, its function in vision or other pathways remains to be
190 determined. Only one of two *peropsin* genes (Tm_08036) appears to be expressed in the *T.*
191 *mercedesae* transcriptome, and it was highly expressed in the female compared to the male
192 (Supplementary Fig. 8). Female may use this peropsin to move out from the brood cell for
193 reproduction. The other components in phototransduction are present in *T. mercedesae*, suggesting
194 that they could be involved in other signaling pathways. In contrast to *T. mercedesae*, *M.*
195 *occidentalis* was reported to contain more molecular components for light perception such as
196 arrestins and INAD and exhibit genuine light-induced behaviors in the absence of eyes [21].
197 Meanwhile, *I. scapularis* contains seven opsins, including orthologs of the insect long-wavelength
198 sensitive visual opsins [28], demonstrating that the tick uses more visual cues for location of mates,
199 hosts and oviposition sites than the mites above.

200 Insect gustatory receptors (GRs) are multifunctional proteins for the perception of taste, airborne
201 molecules, and heat [29]; however, their functions in other arthropods have not been addressed. We
202 found only five GRs in *T. mercedesae* (TmGRs) and their orthologs are absent in *D. melanogaster*
203 (Fig. 3). *I. scapularis* has expanded the specific group of GRs [28], and five TmGRs cluster with the
204 tick's GRs, suggesting that these are expansions specific to Acari. Because they share a common
205 ancestor with the *D. melanogaster* sugar receptor, they could be involved in taste perception (Fig. 3).
206 Among the five TmGRs, one gene (Tm_15249) is likely to be a pseudogene due to internal stop
207 codons in the open reading frame. Expression of only two TmGR genes (Tm_03548 and Tm_09509)
208 was supported by RNA-seq data. Tm_09509 mRNA is highly expressed in adult females and
209 Tm_03548 mRNA is only detected in males at low levels (Supplementary Fig. 9), suggesting that
210 they may respond to different ligands.

211 Ionotropic receptors (IRs) belong to a large family of ligand-gated ion channels, which also
212 include ionotropic glutamate receptors (iGluRs) with the major roles in synaptic transmission. IRs
213 appear to represent protostome-specific ancient olfactory and gustatory receptors [30]. We annotated
214 eight IR and 34 iGluR genes in the *T. mercedesae* genome. In the eight annotated *T. mercedesae* IR
215 (TmIR) genes, Tm_15231 and Tm_15229 are orthologs of DmIR25a and DmIR93a, respectively
216 (Supplementary Fig. 10), which are expressed in the olfactory sensory neurons of *D. melanogaster*
217 antennae [31]. Furthermore, DmIR25a has been recently shown to be involved in fruit fly
218 temperature sensation [32, 33]. The results of qRT-PCR revealed that these two genes are highly
219 expressed in the first legs of *T. mercedesae* (Supplementary Fig. 11), which function as the major
220 sensory organs similar to insect antennae [34]. Thus, these two TmIRs may represent the ancient
221 receptors present in the common ancestor of arthropods. It appears that six other TmIRs have arisen
222 specifically in a mite lineage (Supplementary Fig. 12).

223 Interestingly, there are no OR (olfactory receptor), OBP (odorant binding protein), and CSP
224 (chemosensory protein) genes in the *T. mercedesae* genome (Table 2). Since OR and OBP genes are
225 also absent in *M. occidentalis*, the black-legged tick, the centipede (*Strigamia maritima*), and the

226 water flea (*Daphnia pulex*), these appear to have evolved specifically in insect genomes as
227 previously suggested [35]. Nevertheless, CSP genes must be ancient and may have been specifically
228 lost in the two mite species. Despite of the potential importance of chemical communication for the
229 life cycle [4], *T. mercedesae* has only four functional GRs and eight IRs, but no OR, OBP, or CSP
230 genes. The presence of few orthologs between *T. mercedesae* and *D. melanogaster* suggests that the
231 last common ancestor of arthropods had very few GRs and IRs. These chemoreceptors appear to
232 have expanded in arthropod species in a lineage-specific manner [36]. In fact, Parasitiformes
233 exposed to more variable environments, *i.e.*, *M. occidentalis* and *I. scapularis*, have more GR and IR
234 genes than the more strictly host-dependent *T. mercedesae* (Table 2). Simplified behavioral patterns
235 under a dark and stable environment inside a honey bee colony and capped brood cell may have
236 reduced the number of tools in the sensory system in *T. mercedesae*.

237 **Detoxification system**

238 Three major groups of enzymes have important roles for metabolizing toxic xenobiotics in insects
239 and the acquisition of insecticide resistance; cytochrome P450s (P450s), glutathione-S-transferases
240 (GSTs), and carboxylesterases (CCEs) [37]. P450s and CCEs are also involved in the synthesis and
241 degradation of ecdysteroids, juvenile hormones, pheromones, and neurotransmitters [38, 39].
242 After the actions of P450s and CCEs followed by GSTs, the xenobiotics-derived polar compounds or
243 conjugates can be transported out of the cell by ATP-binding cassette transporters (ABC transporters)
244 [40]. In some cases, ABC transporters and others directly and efficiently transport xenobiotics out of
245 the cell without enzymatic modifications to prevent the exertion of toxicity [40]. Since various
246 natural and synthetic chemical compounds have been used to control honey bee mites, it is of
247 considerable interest to understand how *T. mercedesae* may detoxify such miticides and develop
248 resistance.

249 We manually annotated 56 *T. mercedesae* P450 (TmP450) genes in which 18 appeared to be
250 pseudogenes. In fact, the expression of none of these genes was supported by RNA-seq data. Thus, *T.*
251 *mercedesae* has only 38 apparently functional P450 genes similar to the human louse, *Pediculus*
252 *humanus* [41], and the expression of 36 genes were confirmed by RNA-seq data (Supplementary
253 Table 12). Similar to insect P450s, they are phylogenetically clustered into CYP2, CYP3, CYP4, and
254 mitochondrial clans (Fig. 4). The classification was based on *D. melanogaster* P450s, but only three
255 TmP450 genes (Tm11277, Tm11316, and Tm10252) have *D. melanogaster* P450 (DmP450)
256 orthologs classified as CYP2 and mitochondrial clans (Fig. 4 and Table 3). Thus, only a few P450
257 genes were present in the last common ancestor of arthropods and might be associated with the
258 synthesis and degradation of hormones. In the two large CYP3 and CYP4 clans, DmP450s and the
259 mite P450s are phylogenetically separated, suggesting that they have independently expanded after
260 the split of the ancestors of mites and insects (Fig. 4). All of the TmP450 genes have orthologs in the
261 *M. occidentalis* genome as recently reported [42], but *M. occidentalis* has 12 and 13 more genes than
262 *T. mercedesae* in the CYP2 and CYP3 clans, respectively, by our analysis (Table 3). *T. mercedesae*
263 appears to have lost the CYP3 clan members from the common ancestor of the Parasitiformes (Fig.
264 4) as suggested by CAFE analysis (Supplementary Table 13). Some of the TmP450 genes are
265 differentially expressed between nymph, adult male, and adult female (Supplementary Fig. 12 and
266 Supplementary Table 14), suggesting that they would be involved in the synthesis and degradation of
267 hormones to control molting and sex-specific specific phenotypes of *T. mercedesae*.

268 *T. mercedesae* has 15 GST genes (TmGST) in which eight appear to be pseudogenes without
269 evidences of the mRNA expression in the transcriptomes. This leads to only seven functional
270 TmGST genes with mRNA expression confirmed by RNA-seq data (Supplementary Table 15).
271 According to the reference data sets (*D. melanogaster* and *T. urticae* GSTs), the phylogenetic
272 analysis of TmGSTs revealed the presence of four subfamilies (delta, mu, omega, and kappa), and an
273 unclassified TmGST gene (Supplementary Fig. 13). Members in the mu, delta, epsilon, omega, theta,
274 and zeta GST subclasses have been reported to function in a wide range of detoxification [43].
275 Epsilon, sigma, theta, and zeta subfamilies are absent in both *T. mercedesae* and *M. occidentalis* by
276 our analysis in contrast to the recent report [42]; however, *I. scapularis* contains epsilon and zeta
277 subfamilies and *T. urticae* has the theta subfamily (Supplementary Table 16). This suggests that these
278 three subfamilies have been lost from the *T. mercedesae* and *M. occidentalis* genomes. The full
279 length orthologs of the five TmGST pseudogenes (Tm_05455, Tm_09167, Tm_15202, Tm_15203,
280 and Tm_15206) are present in *M. occidentalis* (Supplementary Fig. 13), suggesting that the delta and
281 mu GST subfamilies have undergone constriction in *T. mercedesae*.

282 Insect CCEs can be divided into 14 subfamilies (A to N) with three major groups based on the
283 functions of dietary detoxification (A-C), hormone and pheromone degradation (D-H), and
284 neurotransmitter degradation (I-N) [44]. We manually annotated 50 *T. mercedesae* CCE genes, in
285 which eight appeared to be pseudogenes without mRNA expression (Supplementary Table 17). The
286 number of functional CCE genes in *T. mercedesae* is thus comparable to that in *M. occidentalis* [42]
287 (Supplementary Table 18). Intriguingly, there are no mite CCEs in the subfamilies AF, H, I, K, and
288 N; however, a massive mite specific expansion is found in the subfamilies J and M by our analysis
289 (Supplementary Fig. 14 and Supplementary Table 18). Only three TmCCE genes (Tm_00126,
290 Tm_05721, and Tm_08305) have *D. melanogaster* orthologs, suggesting that CCE genes have
291 independently duplicated in insects and mites. The expression of some TmCCE genes is biased
292 between the nymph, adult female, and adult male (Supplementary Table 19). Above results
293 demonstrate that *T. mercedesae* contains P450s, GSTs, and CCEs although the number and
294 composition of subfamilies are different from those of other arthropods. Some of these enzymes may
295 engage in detoxifying miticides and other xenobiotics in *T. mercedesae*.

296 We annotated 54 ABC transporter genes in the *T. mercedesae* genome, and the expression of 47
297 genes was confirmed by RNA-seq data (Supplementary Table 20). Similarly, *M. occidentalis*
298 contains 57 ABC transporters that are comparable to those present in *D. melanogaster* (56 genes)
299 (Supplementary Table 20). However, mite-specific expansion is found in the ABCC subfamily, and
300 instead fruit fly-specific expansion is observed in the ABCG subfamily (Supplementary Fig. 15). The
301 ABCC subfamily includes many vertebrate multidrug-resistance associated proteins (MRPs) that
302 extrude drugs with broad specificity [40]; thus, the expanded ABCC subfamily members in *T.*
303 *mercedesae* could be involved in conferring resistance against various miticides. In the fruit fly,
304 expansion has been observed of the ABCG subfamily, which contains the transporters for the uptake
305 of pigment precursors into the cells of the Malpighian tubules and developing compound eyes
306 (Supplementary Fig. 15). Because these mites do not have eyes, fewer numbers of the ABCG
307 transporters would be sufficient. The mites and fruit fly appear to have independently expanded
308 ABCA subfamily members (Supplementary Fig. 15). These results suggest that most of the ABCA
309 and ABCC transporters may carry out different functions in mites and fruit flies. Interestingly, two

310 transporters, Tm_07059 and Tm_14842, form an independent clade separated from eight previously
311 known ABC transporter subfamilies. In cases where the mite ABC transporter genes show biased
312 expression between female, male, and nymph, most of them are highly expressed in either male or
313 nymph compared to female (Supplementary Table 21).

314 **Sex determination genes in *T. mercedesae***

315 Arthropods are known to use various strategies for sex determination [45]. In contrast to *T.*
316 *mercedesae*, which is likely to use haplodiploidy, *M. occidentalis* employs parahaploidy, in which the
317 functional elimination of paternal chromosomes occurs during early embryogenesis resulting in male
318 development [46, 21]. To gain insight into the mechanism of sex determination of *T. mercedesae*, we
319 manually annotated the candidate genes for sex determination in the *T. mercedesae* genome.
320 Similarly to *M. occidentalis* [21], *T. mercedesae* does not contain upstream sex determination genes
321 (*Sex-lethal* and *transformer*) but has the homologs of downstream sex determination genes,
322 *transformer-2*, *dmrt* (doublesex and mab3 related transcription factor), and *intersex*. *T. mercedesae*
323 has the most *dmrt* genes of the arthropods that we tested (Supplementary Table 22) and has two extra
324 *dsx* genes compared to *M. occidentalis* (Supplementary Fig. 16). The Dmrt93B ortholog is present in
325 *T. mercedesae* (Tm_07872) but not in *M. occidentalis* (Supplementary Fig. 16), and all of the *dmrt*
326 genes are highly expressed in the male (Supplementary Fig. 17). These results suggest that *T.*
327 *mercedesae* and *M. occidentalis* may use a different set of genes for sex determination.

328 **Comparison of gene expression profiles between nymphs and adult males and females**

329 Comparison between adult male and female transcriptomes and proteomes revealed that
330 histone-lysine-*N*-methyltransferase gene family and N-acetyltransferase *gcn5* gene family were
331 highly expressed in the male compared to the female (Fig. 5, Supplementary file 1, and
332 Supplementary Table 23), suggesting that the male mite may mostly depend on histone modifications
333 for the epigenetic control of gene expression. This could be due to the ploidy compensation between
334 males with haploid genomes and females with diploid genomes. At the protein level, males displayed
335 overrepresentation of 26S proteasome subunits and a 17-beta-hydroxysteroid dehydrogenase (Fig. 5),
336 which accords with the importance of the ubiquitin-proteasome system in sperm maturation [47] and
337 a potential role for ecdysteroids in sexual maturation of *T. mercedesae* [48]. The female mite highly
338 expresses the vitellogenin gene family and cathepsin L-like proteases (Fig. 5 and Supplementary
339 Table 23). This is consistent with active oogenesis in female mites, since both vitellogenin protein
340 and Nanos mRNA would be deposited in the oocyte; while cathepsin L proteases may have a critical
341 role in yolk processing as in *C. elegans* [49]. The results of above transcriptome and proteome
342 analyses are not identical but a concordant set of 74 and 13 genes are up-regulated in the male and
343 females, respectively. Comparison between adult female and nymph transcriptomes demonstrated
344 that 46 out of the 125 cuticle protein gene families, 13 out of 24 chitin binding domain-containing
345 protein gene families, and nine out of 16 chitinase gene families are expressed at a higher level in
346 nymphs than in adult females (Supplementary Table 24), indicating that chitin metabolism as well as
347 exoskeleton formation by molting is stimulated in the nymph. The nymph also highly expresses 18
348 out of 29 protocadherin/fat gene families and 18 out of 44 epidermal growth factor-related receptor
349 gene families. These are likely to be involved in cell-cell adhesion and cell proliferation associated
350 with the increase of cell number in nymph. Consistent with above results, GO analysis of genes
351 highly expressed in nymphs compared to the adult females demonstrated that many GO terms related

352 to cuticle formation and appendage morphogenesis are enriched (Supplementary Table 25).

353 **Symbiotic bacteria and infecting virus**

354 Several bacteria have been shown to associate with mites and ticks [17, 50, 51]; however, bacteria
355 associated with honey bee mites have not yet been fully investigated [11]. We thus attempted to
356 identify any bacteria associated with *T. mercedesae* by filtering the bacteria-derived DNA contigs
357 during the mite genome assembly. In the male and female GC%-coverage plots, some contigs were
358 initially annotated as bacterial DNA in the major blue blob, and most of these were identified to
359 contain *Wolbachia* sequences by BLASTN searches (Fig. 6). We confirmed that parts of *Wolbachia*
360 genes are integrated into the mite genome by testing two genomic contigs using PCR with two sets
361 of primers (one primer located in the mite gene, and the other in the *Wolbachia* gene)
362 (Supplementary Fig. 18A and B). This phenomenon of nuclear *Wolbachia* transfers, or *nuwts*, has
363 been observed widely in other arthropods and in nematodes [52], although to the best of our
364 knowledge, this is the first report for a chelicerate. It suggests that *T. mercedesae* or the ancestor had
365 *Wolbachia* as the endosymbiont in the past. Meanwhile, we extracted all reads mapped to the red
366 blob (bacterial origin) in the female plot (Fig. 6) and re-assembled them into 96 contigs. We
367 annotated 751 protein-coding genes from the 81 contigs and found that 667 of these show high
368 similarity to those of *Rickettsiella grylli* with an average identity of 79%. The rest of the 84
369 protein-coding genes showed similarity to 20 other bacteria species, such as *Diplorickettsia*
370 *massiliensis* and *Legionella longbeachae*. This demonstrates that a close relative of *R. grylli*
371 associates with female but not male *T. mercedesae*. *Rickettsiella* is an intracellular
372 gamma-proteobacterium associated with a wide range of different arthropods without major
373 pathogenicity to the host [53]. *Wolbachia* endosymbiont in the past may have been replaced by a
374 species related to *R. grylli* in *T. mercedesae*. The potential effects on *T. mercedesae* as well as the
375 potential for transmission to the honey bee remain to be determined. Since we did not find any DNA
376 sequences of actinomycete species in our sequence reads, the two major ectoparasitic mites of honey
377 bee (*V. destructor* and *T. mercedesae*) do not appear to share the same bacteria [11]. Nevertheless,
378 both mites do not contain common arthropod gut bacteria, suggesting that they are not essential for
379 the honey bee mites.

380 We also assembled DWV RNA in the adult male and female, as well as nymph, transcriptomes
381 (Supplementary Table 26). This is consistent with previous reports [54, 6, 7]; however, our data
382 expand the infected stages to include the adult males and nymphs. DWV sequence reads represented
383 one third of the whole RNA-seq data, and these very high levels of DWV RNA were further
384 confirmed by qRT-PCR (Supplementary Table 27). The proteomic analysis of females and males
385 recovered many peptides derived from the capsid (structural) proteins, but very few peptides from
386 the non-structural proteins of DWV, demonstrating that the majority of DWV associated with the
387 mites exists as mature virions (Supplementary Fig. 19). Similar observations were also reported for *V.*
388 *destructor* [55]. We assembled three full length DWV RNA genomes and found that they are
389 phylogenetically clustered with type A DWV [56] (Fig. 7). Thus, *T. mercedesae* may spread the
390 specific strain of DWV (type A in this study) to honey bees as suggested for *V. destructor* [57].
391 Considering that *T. mercedesae* was unlikely to carry DWV when associated with the original host,
392 *A. dorsata*, DWV infection could impose a negative impact on the mite. It will be crucial to
393 understand the nature of interactions between honey bee, mite, and DWV to measure the impact of *T.*

394 *mercedesae* infestation on honey bee colonies. However, in contrast to *V. destructor*, we did not
395 detect baculoviruses in either the genome and transcriptome sequences [11].
396

397 **Conclusions**

398 *T. mercedesae* has a very specialized life history and habitat as an ectoparasitic mite strictly
399 depending on honey bees in a colony with closed and stable environment. Thus, comparison of the
400 genome and transcriptome sequences with those of a free-living mite and a tick has revealed the
401 specific features of the genome shaped by interaction with the honey bee and colony environment.

402 Our key findings are the followings;

- 403 1) Amino acid substitutions have been accelerated within the conserved core genes of *T. mercedesae*
404 and *M. occidentalis*
- 405 2) *T. mercedesae* has undergone the least gene family expansion and contraction between the seven
406 arthropods we tested
- 407 3) The numbers of HSP70 family genes and sensory system genes are reduced
- 408 4) *T. mercedesae* may have evolved a specialized cuticle and water homeostasis mechanisms, as well
409 as epigenetic control of gene expression for ploidy compensation between male and female
- 410 5) *T. mercedesae* contains all gene sets required to detoxify xenobiotics, enabling it to be miticide
411 resistant
- 412 6) *T. mercedesae* is closely associated with a symbiotic bacterium (*Rickettsiella grylli*-like) and
413 DWV, the most prevalent honey bee virus.

414
415 Manipulation of symbiotic *R. grylli*-like bacteria in the female mites may give the opportunity to
416 control *T. mercedesae* in the future. Our *T. mercedesae* datasets, alongside published *V. destructor*
417 genome and transcriptome sequences, not only provide insights into mite biology, but may also help
418 to develop measures to control the most serious pests of the honey bee.
419

420 **Methods**

421 **Mite sample collection**

422 Based on the morphological and ethological characteristics [58], adult males and females as well as
423 nymphs of *T. mercedesae* were identified and collected from a single honey bee colony for the flow
424 cytometric analysis and Illumina sequencing (genome and transcriptome). Meanwhile, the adult
425 females #2 sample (Supplementary Table 1) was collected from a different colony. Both colonies
426 were obtained from a beekeeper in Jiangsu Province, China. The mites collected for genome
427 sequencing and proteomic characterization were stored in acetone at 4°C until use. The mites used
428 for RNA-seq were sorted at -80°C before the transport.

429 **Genome sequencing**

430 Before DNA extraction, the mite bodies were carefully washed twice with acetone to remove any
431 non-target organisms that might adhere on the mite surface. Subsequently, a single male and a single
432 female mite were air dried (15 min) and individually triturated in 180 µL of lysozyme buffer (1M
433 Tris-HCl, 0.5M EDTA, 1.2% Triton X-100, and 0.02% lysozyme) with a tissuelyser II (Qiagen,
434 Valencia, USA) using a 3 mm stainless steel bead at 25,000 motions/min for 30 sec. After incubating
435 the samples at 37 °C for 30 min, total DNA was extracted from each of the triturated samples with
60

436 DNeasy Blood and Tissue kit (Qiagen) by following the manufacturer's spin-column protocol for
437 animal tissue. To maximize the yield of DNA extraction, two successive elution steps, each with 50
438 µl elution buffer, were performed. The DNA concentrations were determined by spectrophotometry,
439 a sensitive and commonly used fluorescent dye assay (Qubit® dsdna BR assay, Life Technologies
440 Europe, Naerum, Denmark) according to the manufacturer's instructions. Two paired-end Illumina
441 DNA libraries were constructed with the male and female total genomic DNA samples (30 ng each)
442 using a Nextera DNA sample preparation kit (Illumina, Great Chesterford, United Kingdom). The
443 DNA libraries were then quality controlled and sequenced with Illumina Hiseq 2500 system using
444 two individual lanes in the Centre for Genomic Research at the University of Liverpool. The raw
445 fastq files were trimmed to remove Illumina adapter sequences using Cutadapt (v1.2.1) [59]. The
446 option “-O 3” was set, so the 3' end of any reads which matched the adapter sequence over at least 3
447 bp was trimmed off. The reads were further trimmed to remove low quality bases, using Sickle
448 (v1.200) [60] with a minimum window quality score of 20. After trimming, reads shorter than 10 bp
449 were removed.

450 **Transcriptome sequencing**

451 Male, female and nymph mites were shipped to BGI-Shenzhen with dry ice for total RNA extraction,
452 polyA⁺ RNA enrichment, cDNA library preparation, and Illumina Hiseq 2000/4000 sequencing.
453 Total RNA (Supplementary Table 1) was extracted from a pool of 20~30 mites using Trizol reagent
454 (Qiagen) and treated with DNase I (Qiagen). Next, polyA⁺RNA was isolated by magnetic beads with
455 oligo (dT) and digested to short fragments by mixing with the fragmentation buffer, and then the
456 cDNA was synthesized. The short DNA fragments were purified and resolved with EB buffer for
457 end reparation and single nucleotide A (adenine) addition followed by ligation with adapters. DNA
458 fragments suitable for sequencing were then selected for the PCR amplification. After QC steps,
459 Illumina Hiseq 2000 system was used to sequence the libraries of adult males #1 (in two lanes), adult
460 females #1 (in two lanes), nymphs #1 (in two lanes) and adult females #2 (in a single lane), whereas
461 adult males #2 and nymphs #2 were sequenced with Illumina Hiseq 4000 system in a single lane.
462 Raw reads were trimmed and filtered by internal tools of BGI-Shenzhen.

463 **Estimation of genome size and ploidy of *T. mercedesae***

464 Nuclear DNA contents of *T. mercedesae* males and females were estimated by a method of
465 propidium iodide staining followed by flow cytometry [19]. Nuclei were isolated from ten *T.*
466 *mercedesae* adult males and females, the heads of ten *D. melanogaster* females (1C = 175Mb) [61]
467 and the brain of a honey bee worker (1C = 262 Mb) [62] by homogenizing each sample with 1 mL of
468 a cold Galbraith buffer (30 mM sodium citrate, 18 mM MOPS (3-morpholinopropanesulfonic acid),
469 21 mM MgCl₂, 0.1% Triton X-100, 1 mg/L RNase A) using a loose pestle. The cellular debris were
470 removed by filtering through 20 µm nylon mesh. Stained nuclei from adult male and female mites
471 were independently analyzed with two reference standards using a BD FACS flow cytometer (BD
472 Biosciences, San Jose, CA). Nuclear genome size was then calculated according to the following
473 formula: Sample nuclear DNA content = (Mean peak of sample/Mean peak of reference standard) ×
474 nuclear DNA content of reference standard. We estimated the genome size by analyzing the
475 frequency of *k*-mers counted by Jellyfish [63] with the following formula [64]: Estimated genome
476 size (bp) = total number of *k*-mer/the maximal frequency. The ploidy is the ratio of nuclear DNA
477 content to genome size.

478 **De novo assembly of genomic DNA**

479 Prior to assembly, we discarded all male and female sequencing reads aligned to honey bee genome
480 sequence by Bowtie 2 (v2.2.1) [65]. The unaligned male and female reads were then extracted by
481 bam2fastq (v1.1.0) and assembled individually by Velvet v1.2.07 [66] into preliminary contigs with
482 their best k-mers and parameters of ‘-min_contig_lgth=200 and -ins_length 1105 (male)/939
483 (female)’. DNA sequences derived from non-targets such as bacteria and mitochondria were filtered
484 out based on the preliminary assemblies of male and female genome sequences using a GC-coverage
485 (proportion of GC bases and node coverage) plot-based method by blobtools (v0.9.19) [67] (Fig. 6),
486 resulting in total 400,520,654 and 453,725,764 “clean reads” for male and female mite, respectively.
487 The male “clean reads” were re-assembled and optimized up to scaffold level using the
488 VelvetOptimiser (v2.2.5) with the velvet parameters set to ‘-min_contig_lgth 200 and -ins_length
489 1105’.

490 **Genome annotation**

491 To find, classify and mask repeated sequences in the assembled male genome, a *de novo* repeat
492 library was first built using Repeatmodeler (A. F. A. Smit and P. Green, unpublished) with
493 ‘-database’ function followed by Repeatmasker (A. F. A. Smit and P. Green, unpublished) using
494 default setting for *de novo* repeated sequences prediction. Then, a homology-based prediction of
495 repeated sequences in the genome was achieved using Repeatmasker with default setting to search
496 against RepBase repeat library issued on January 13, 2014. For non-interspersed repeated sequences,
497 we ran Repeatmasker with the ‘-noint’ option, which is specific for simple repeats, micro satellites,
498 and low-complexity repeats.

499 RNA-seq reads obtained from all samples were aligned to the masked genomic scaffolds to
500 determine the exon-intron junctions using Tophat (v2.0.11) with default setting [69]. Cufflinks (v0.8.2)
501 [70] used the spliced alignments with default setting to reconstruct 44,614 transcripts from which
502 12,298 transcripts with intact coding sequences were selected by a Perl script developed by Liu et al.
503 [71]. Thee *ab initio* gene prediction programs, including Augustus (v3.0.3) [72], SNAP (v2013-11-29)
504 [73] and Genemark (v2.3e) [74] were used for *de novo* gene predictions. Augustus and SNAP were
505 trained based on the selected intact coding sequences with default setting, whereas GeneMark [74]
506 was self-trained with ‘--BP OFF’ option. We ran Augustus, SNAP, and Genemark with default
507 setting, and predicted 32,561, 67,258, and 79,928 gene models in the masked genomic scaffolds,
508 respectively (Supplementary Table 2).

509 We also generated an integrated gene sets using MAKER v2.31.4 [75] pipeline. The MAKER
510 pipeline runs Augustus, SNAP and Genemark to produce *de novo* gene predictions, and integrates
511 them with the evidence based predictions. They were generated by aligning all Cufflinks assembled
512 transcript sequences and the invertebrate RefSeq protein sequences (downloaded on May 17, 2014
513 from NCBI) to the masked male mite genome by BLASTN and BLASTX, respectively. The
514 MAKER pipeline was run with ‘-RM_off’ option to turn all repeat masking options off, and all
515 parameters in control files were left with their default settings.

516 Genes identified by *de novo* prediction, which did not overlap with any genes in the integrated
517 gene sets, were also added to the final gene set if they showed significant hits (BLASTP E-value <
518 1e-5) to SwissProt proteins or could be annotated by Interproscan (v4.8) [76] with InterPro
519 superfamily database (v43.1) using ‘-appl superfamily -nocrc’ options.

520 **ncRNA annotation**

521 In this analysis, we annotated four types of ncRNA: transfer RNA (tRNA), ribosomal RNA (rRNA),
522 microRNA, and small nuclear RNA (snRNA). Genes encoding tRNA were predicted by tRNAScan-SE
523 (v1.3.1) [77] with eukaryote parameters, and rRNA genes were identified by aligning the rRNA
524 template sequences from invertebrates (database: SILVA 119) to the *T. mercedesae* genomic DNA
525 using BLASTN with an E-value cutoff of 1e-5. Genes encoding miRNA and snRNA were inferred
526 by the Infernal software (v1.1.1) [78] using release 12 of the Rfam database with ‘--cut_tc’ option.

527 **Protein functional annotation**

528 We performed the initial and principal domain annotation with the Pfam database (release 27) using
529 the hmmscan in HMMER v3.1b1 with default settings. Additional domains (superfamily, Gene3d,
530 Tigrfams, Smart, Prosite, and Prints domain models) and domain/motif based GO term were
531 assigned using InterProScan search against InterPro database (v43.1) with ‘-cli -nocrc -goterms
532 -iprlookup’ options.

533 We used Blast2GO pipeline (v2.5) [79] to further annotate proteins by Gene Ontology (GO)
534 terms. In the first step, we searched the nr database with BLASTP using a total of 15,190 protein
535 sequences as queries. The E-value cutoff was set at 1e-6 and the best 20 hits were collected for
536 annotation. Based on the BLAST results, Blast2GO pipeline then predicted the functions of proteins
537 to assign GO terms, and merged the InterProScan deduced domain/motif based GO terms into these
538 BLAST based annotations.

539 The metabolic pathway was constructed based on the KAAS (KEGG Automatic Annotation
540 Server) online server [80] using the recommended eukaryote sets, all other available insects, and *I.*
541 *scapularis*. The pathways in which each gene product might be involved were derived from the best
542 KO hit with BBH (bi-directional best hit) method.

543 **GO enrichment**

544 We performed the GO enrichment analyses of gene sets with Fisher's exact test embedded in the
545 Blast2GO desktop version (v2.8). If not specifically stated, the *P*-values were corrected according to
546 the critical FDR. The enrichments were tested by comparing the GO terms with the pooled set of GO
547 terms of all *T. mercedesae* proteins.

548 **Species tree phylogenetics**

549 We first aligned orthologous protein sequences with Mafft (v7.012b) [81] or Kalign (v2.0) [82], and
550 then used Gblocks (v0.91b) [83] to automatically eliminate the divergent regions or gaps prior to
551 phylogenetic analysis. However, we manually trimmed the aligned sequences for big gene sets. The
552 best substitution models of amino acid substitution were determined for the alignments by Prottest
553 (v3.4) with parameters set to “-all-matrices, -all-distributions, -AIC” [84]. Then, phylogenetic trees
554 were constructed using maximum likelihood methods (Phyml, v3.1) [85] or Bayesian methods
555 (MrBayes, v3.2.3) [86]. In addition, a neighbor-joining method was also used for building the
556 distance-based trees using MEGA (v6.06) [87].

557 **Protein data sets of reference genomes**

558 Protein data sets of the following arthropod genomes were used as references: *D. melanogaster* (fruit
559 fly; GOS release: 6.03) [88], *A. mellifera* (honey bee; GOS release: 3.2) [62], *T. urticae* (spider mite;
560 GOS release: 20140320) [15], *Stegodyphus mimosarum* (velvet spider; GOS release: 1.0) [89], *I.*
561 *scapularis* (black-legged tick; GOS release: 1.4) [28], *M. occidentalis* (predatory mite; GOS release:

562 1.0) [21]. *Caenorhabditis elegans* (nematode; GOS release: WS239) [90] was used as the outgroup.
563 Domain, GO, and KEGG annotation of proteins in the reference species (if required) was conducted
564 using the same methods as those used for *T. mercedesae*.

565 **Gene family phylogenetics**

566 Since the rapid evolution of acariform mites may challenge phylogenetic analyses due to long-branch
567 attraction [91], we used a very strict E-value (1e-50) when performing a reciprocal BLASTP to gate
568 out the most variant orthologous genes across all genomes tested. The reciprocal BLAST search
569 resulted in identification of a total of 926 highly conserved one-to-one orthologs in all eight genomes.
570 Each of these orthologous groups was aligned using Mafft in “-auto” option. These alignments were
571 trimmed by Gblocks and concatenated into the unique protein superalignments. ProtTest determined
572 the best-fit substitution model of LG with invariant sites (0.109) and gamma (0.913) distributed rates
573 using parameters as above before conducting the phylogenetic analysis with PhymI.

574 **Analysis of gene family expansion and positive selection**

575 Orthologous gene families between *T. mercedesae* and six reference arthropods were defined based
576 on OrthoMCL (v1.4) [93] clustering. We used CAFE (v3.1) [94] to infer the gene family expansion
577 and contraction in *T. mercedesae* against all reference arthropods or against Parasitiformes (*I.*
578 *scapularis* and *M. occidentalis*). The ultrametric species tree used in CAFE analyses was created as
579 described in Gene family phylogenetics section.

580 We also calculated ω (dN/dS) ratios for 1,865 one-to-one orthologs defined by OrthoMCL using
581 codeml in the PAML package with the free-ratio model. Branches with $\omega > 1$ are considered under
582 positive selection. The null model used for branch test was the one-ratio model, where ω was the
583 same for all branches. The null model used for branch test was the one-ratio model (nssites = 0;
584 model = 0) where ω was the same for all branches. Kappa and omega values were automatically
585 estimated from the data, when clock was set to be entirely free to change among branches. *P*-value
586 was determined twice using the log-likelihood difference between the two models compared to χ^2
587 distribution with the difference in number of parameters between one-ratio and free-ratio models. To
588 estimate significance with the *P*-value, likelihood-ratio test (LRT) was used to compare lnL values for
589 each model and test if they are significantly different. The differences in log-likelihood values
590 between two models were compared to chi-square distribution with degree of freedom equal to the
591 difference in the number of parameters for two models. Measurement of dS was assessed for
592 substitution saturation, and only dS values < 3.0 were maintained in the analysis for positive
593 selection. Genes with high ($\omega > 10$) were also discarded.

594 **De novo transcriptome assembly and estimation of the transcript abundance**

595 All RNA-seq reads mapped to the honey bee transcripts were filtered out first. Then, all RNA-seq
596 samples in Supplementary Table 1 were individually *de novo* assembled by Trinity (v20131110) [95]
597 with default setting. We used a RSEM [96] software package to estimate the expression levels
598 (abundance) of *de novo* assembled transcripts and isoforms with default setting.

599 **Analysis of RNA-seq data**

600 After further removing the RNA-seq reads corresponding to DWV sequence, we aligned the cleaned
601 reads to the assembled *T. mercedesae* genome using Tophat with default setting. Then, Htseq-count
602 in the Htseq Python package (v0.6.1) [97] was used to obtain raw read counts, with the default
603 union-counting mode and option ‘-a’ to specify the minimum score for the alignment quality. The

604 raw read count for each sample was then subject to further differential expression analysis using the
605 EdgeR (v3.0) Bioconductor package [98]. We excluded mRNAs without at least one count per
606 million in the replicates (low overall sum of counts) from the analyses as previously suggested [99].
607 We then normalized the library sizes of all samples according to the trimmed mean of M-values
608 method, and dispersion was estimated from the replicates using the quantile-adjusted conditional
609 maximum likelihood method. Pairwise comparisons of differential gene expression between the
610 RNA-seq samples were performed using the function of Exact test. We used the corrected FDR
611 P -value < 0.01 , and $\log_{2}FC > 1$ and $\log_{2}FC < -1$ cut-offs for significance.

612 **qRT-PCR**

613 We carried out qRT-PCR reactions, each in triplicate, using an Applied Biosystems 7500 Fast
614 Real-Time PCR System and 2X KAPA SYBR FAST qPCR Master Mix (KAPA Biosystems Woburn,
615 MA). To perform the absolute quantification of DWV RNA, we first prepared standard curves for
616 DNA corresponding to DWV target RNA. The target DNA was prepared by PCR followed by the gel
617 extraction. The DNA concentration was measured using Nanodrop 2000 spectrophotometer (Thermo
618 Scientific, USA) to calculate the original copy number by a formula; Copy number = DNA
619 concentration (ng/ μ l) $\times 6.02 \times 10^{23}$ (copies/mol) / length (bp) $\times 6.6 \times 10^{11}$ (ng/mol), in which
620 6.6×10^{11} ng/mol is the average molecular mass of one base pair, and 6.022×10^{23} copies/mol is the
621 Avogadro's number. Linear standard curves were then generated using target DNA of 10^5 – 10^9 copy
622 number per reaction followed by plotting the Ct values against log values of the copy number. After
623 reverse transcription, the copy number of target RNA in a sample was estimated using the standard
624 curve above. To carry out the relative quantification, we compared the relative expression levels of
625 the target mRNA to *Ef-1 α* mRNA as the internal reference using the $2^{-\Delta\Delta C_t}$ method. All primers used
626 for qRT-PCR are listed in Supplementary Table 28.

627 **Proteomic analysis**

628 Pools of male or female ites were lysed by sonication in 0.1 % (w/v) Rapigest (Waters MS
629 technologies) in 50 mM ammonium bicarbonate. Samples were heated at 80 °C for 10 min, reduced
630 with 3 mM DTT at 60 °C for 10 min, cooled, then alkylated with 9 mM iodoacetamide (Sigma) for
631 30 min (room temperature) protected from light; all steps were performed with intermittent
632 vortex-mixing. Proteomic-grade trypsin (Sigma) was added at a protein:trypsin ratio of 50:1 and
633 incubated at 37 °C overnight. Rapigest was removed by adding TFA to a final concentration of 1 %
634 (v/v) and incubating at 37 °C for 2 hours. Peptide samples were centrifuged at 12,000 $\times g$ for 60 min
635 (4 °C) to remove precipitated Rapigest. The peptide supernatant was desalted using C₁₈
636 reverse-phase stage tips (Thermo Scientific) according to the manufacturer's instructions. Samples
637 were desalted and reduced to dryness as above and re-suspended in 3 % (v/v) acetonitrile, 0.1 % (v/v)
638 TFA for analysis by MS.

639 Peptides were analysed by on-line nanoflow LC using the nanoACQUITY-nLC system (Waters
640 MS technologies) coupled with Q-Exactive mass spectrometer (Thermo Scientific). Samples were
641 loaded on a 50cm Easy-Spray column with an internal diameter of 75 μ m, packed with 2 μ m C₁₈
642 particles, fused to a silica nano-electrospray emitter (Thermo Scientific). The column was operated at
643 a constant temperature of 35 °C. Chromatography was performed with a buffer system consisting of
644 0.1 % formic acid (buffer A) and 80 % acetonitrile in 0.1 % formic acid (buffer B). The peptides
645 were separated by a linear gradient of 3.8 – 50 % buffer B over 90 minutes at a flow rate of 300

646 nl/min. The Q-Exactive was operated in data-dependent mode with survey scans acquired at a
647 resolution of 70,000. Up to the top 10 most abundant isotope patterns with charge states +2, +3
648 and/or +4 from the survey scan were selected with an isolation window of 2.0Th and fragmented by
649 higher energy collisional dissociation with normalized collision energies of 30. The maximum ion
650 injection times for the survey scan and the MS/MS scans were 250 and 50 ms, respectively, and the
651 ion target value was set to 1E6 for survey scans and 1E5 for the MS/MS scans. Repetitive
652 sequencing of peptides was minimized through dynamic exclusion of the sequenced peptides for 20s.

653 Thermo RAW files were imported into Progenesis LC-MS (version 4.1, Nonlinear Dynamics).
654 Runs were time aligned using default settings and using an auto selected run as reference. Peaks
655 were picked by the software using default settings and filtered to include only peaks with a charge
656 state between +2 and +7. Spectral data were converted into .mgf files with Progenesis LC-MS and
657 exported for peptide identification using the Mascot (version 2.3.02, Matrix Science) search engine.
658 Tandem MS data were searched against translated ORFs from *T. mercedesae*, *Apis mellifera*
659 (OGSv3.2) [101] and Deformed Wing Virus (Uniprot 08 2016) (total; 30,666 sequences; 12,194,618
660 residues). The search parameters were as follows: precursor mass tolerance was set to 10 ppm and
661 fragment mass tolerance was set as 0.01Da. Two missed tryptic cleavages were permitted.
662 Carbamidomethylation (cysteine) was set as a fixed modification and oxidation (methionine) set as
663 variable modification. Mascot search results were further validated using the machine learning
664 algorithm Percolator embedded within Mascot. The Mascot decoy database function was utilised and
665 the false discovery rate was < 1%, while individual percolator ion scores >13 indicated identity or
666 extensive homology ($P < 0.05$). Mascot search results were imported into Progenesis LC-MS as
667 XML files. Peptide intensities were normalised against the reference run by Progenesis LC-MS and
668 these intensities are used to highlight relative differences in protein expression between samples. The
669 mass spectrometry proteomics data have been deposited to the ProteomeXchange Consortium via the
670 PRIDE [102] partner repository with the dataset identifier PXD004997.

672 **Data availability**

673 All sequence data we obtained and analyzed are deposited under the project accession number
674 PRJNA343868 in NCBI.

676 **Additional files**

677 Supplementary file 1

678 Supplementary Tables

679 Supplementary Figures

681 **Abbreviations**

682 CCE: Carboxylesterase; CSP: Chemosensory protein; CYP: Cytochrome P450; ABC transporter:
683 ATP-binding cassette transporter; GR: Gustatory receptor; GST: Glutathione-S-transferase; IR:
684 Ionotropic receptor; OBP: Odorant binding protein; OR: Olfactory receptor; P450: Cytochrome P450;
685 DWV: Deformed wing virus; MS: Mass spectrometry.

687 **Competing interests**

690

688 We declare no competing interests.

689

690 **Authors' contributions**

691 XD conducted all experiments except the proteomic analyses which were carried out by SDA and
692 DX. TK, ACD, and BLM planned and supervised the research. XD and TK wrote the manuscript,
693 which was revised by ACD and BLM.

694

695 **Acknowledgements**

696 This work was supported in part by 2012 Suzhou Science and Technology Development Planning
697 Programme (Grant#: SYN201213) and Jinji Lake Double Hundred Talents Programme to TK. We
698 thank the Centre for Genomic Research at the University of Liverpool for *Tropilaelaps* mite genome
699 sequencing and Frances Blow for helping to construct the DNA libraries. We are grateful to local bee
700 keepers in Jiangsu province for providing honey bee colonies.

701

702 **References**

- 703 1. Vanengelsdorp D, Meixner MD. A historical review of managed honey bee populations in Europe
704 and the United States and the factors that may affect them. *J Invertebr Pathol.* 2010;103 Suppl
705 1:S80-95. doi:10.1016/j.jip.2009.06.011.
- 706 2. Evans JD, Schwarz RS. Bees brought to their knees: microbes affecting honey bee health. *Trends*
707 *Microbiol.* 2011;19(12):614-20. doi:10.1016/j.tim.2011.09.003.
- 708 3. Rosenkranz P, Aumeier P, Ziegelmann B. Biology and control of *Varroa destructor*. *J Invertebr*
709 *Pathol.* 2010;103 Suppl 1:S96-119. doi:10.1016/j.jip.2009.07.016.
- 710 4. Anderson DL, Roberts JMK. Standard methods for *Tropilaelaps* mites research. *J Apic Res.*
711 2013;52(4). doi:10.3896/ibra.1.52.4.21.
- 712 5. Sammataro D, Gerson U, Needham G. Parasitic mites of honey bees: Life history, implications,
713 and impact. *Annu Rev Entomol.* 2000;45:519-48. doi:10.1146/annurev.ento.45.1.519.
- 714 6. Dainat B, Ken T, Berthoud H, Neumann P. The ectoparasitic mite *Tropilaelaps mercedesae* (Acari,
715 Laelapidae) as a vector of honeybee viruses. *Insectes Sociaux.* 2009;56(1):40-3.
716 doi:10.1007/s00040-008-1030-5.
- 717 7. Forsgren E, de Miranda JR, Isaksson M, Wei S, Fries I. Deformed wing virus associated with
718 *Tropilaelaps mercedesae* infesting European honey bees (*Apis mellifera*). *Exp Appl Acarol.*
719 2009;47(2):87-97. doi:10.1007/s10493-008-9204-4.
- 720 8. Khongphinitbunjong K, de Guzman L, Tarver M, Rinderer T, Chantawannakul P. Interactions of
721 *Tropilaelaps mercedesae*, honey bee viruses and immune response in *Apis mellifera*. *J Apic Res.*
722 2015;54(1):40-7. doi:10.1080/00218839.2015.1041311.
- 723 9. Khongphinitbunjong K, Neumann P, Chantawannakul P, Williams G. The ectoparasitic mite
724 *Tropilaelaps mercedesae* reduces western honey bee, *Apis mellifera*, longevity and emergence weight,
725 and promotes Deformed wing virus infections. *J Invertebr Pathol.* 2016;137:38-42.
726 doi:10.1016/j.jip.2016.04.006.
- 727 10. Oldroyd BP. Coevolution while you wait: *Varroa jacobsoni*, a new parasite of western honeybees.
728 *Trends Ecol Evol.* 1999;14(8):312-5.
- 729 11. Cornman SR, Schatz MC, Johnston SJ, Chen YP, Pettis J, Hunt G et al. Genomic survey of the

60

61

62

63

64

65

- ectoparasitic mite *Varroa destructor*, a major pest of the honey bee *Apis mellifera*. *BMC Genomics*. 2010;11:602. doi:10.1186/1471-2164-11-602.
12. Parra G, Bradnam K, Korf I. CEGMA: a pipeline to accurately annotate core genes in eukaryotic genomes. *Bioinformatics*. 2007;23(9):1061-7. doi:10.1093/bioinformatics/btm071.
13. Simão FA, Waterhouse RM, Ioannidis P, Kriventseva EV, Zdobnov EM. BUSCO: assessing genome assembly and annotation completeness with single-copy orthologs. *Bioinformatics*. 2015;31(19):3210-2. doi:10.1093/bioinformatics/btv351.
14. Xu X, Pan S, Cheng S, Zhang B, Mu D, Ni P et al. Genome sequence and analysis of the tuber crop potato. *Nature*. 2011;475(7355):189-95. doi:10.1038/nature10158.
15. Grbic M, Van Leeuwen T, Clark R, Rombauts S, Rouze P, Grbic V et al. The genome of *Tetranychus urticae* reveals herbivorous pest adaptations. *Nature*. 2011;479(7374):487-92. doi:10.1038/nature10640.
16. Jeyaprakash A, Hoy MA. The nuclear genome of the phytoseiid *Metaseiulus occidentalis* (Acari: Phytoseiidae) is among the smallest known in arthropods. *Exp Appl Acarol*. 2009;47(4):263-73. doi:10.1007/s10493-008-9227-x.
17. Chan TF, Ji KM, Yim AK, Liu XY, Zhou JW, Li RQ et al. The draft genome, transcriptome, and microbiome of *Dermatophagoides farinae* reveal a broad spectrum of dust mite allergens. *J Allergy Clin Immunol*. 2015;135(2):539-48. doi:10.1016/j.jaci.2014.09.031.
18. Rider SD, Morgan MS, Arlian LG. Draft genome of the scabies mite. *Parasit Vectors*. 2015;8:585. doi:10.1186/s13071-015-1198-2.
19. Geraci NS, Spencer Johnston J, Paul Robinson J, Wikel SK, Hill CA. Variation in genome size of argasid and ixodid ticks. *Insect Biochem Mol Biol*. 2007;37(5):399-408. doi:10.1016/j.ibmb.2006.12.007.
20. Gu XB, Liu GH, Song HQ, Liu TY, Yang GY, Zhu XQ. The complete mitochondrial genome of the scab mite *Psoroptes cuniculi* (Arthropoda: Arachnida) provides insights into Acari phylogeny. *Parasit Vectors*. 2014;7:340. doi:10.1186/1756-3305-7-340.
21. Hoy MA, Waterhouse RM, Wu K, Estep AS, Ioannidis P, Palmer WJ et al. Genome Sequencing of the Phytoseiid Predatory Mite *Metaseiulus occidentalis* Reveals Completely Atomized Hox Genes and Superdynamic Intron Evolution. *Genome Biol Evol*. 2016;8(6):1762-75. doi:10.1093/gbe/evw048.
22. Stern D. The genetic causes of convergent evolution. *Nature Rev Genet*. 2013;14(11):751-64. doi:10.1038/nrg3483.
23. Charles JP. The regulation of expression of insect cuticle protein genes. *Insect Biochem Mol Biol*. 2010;40(3):205-13. doi:10.1016/j.ibmb.2009.12.005.
24. Kaufman W, Aeschlimann A, Diehl P. Regulation of body volume by salivation in a tick challenged with fluid loads. *Am J Physiol*. 1980;238(1):R102-R12.
25. Sauer J, Mcswain J, Bowman A, Essenberg R. Tick salivary-gland physiology. *Annu Rev Entomol*. 1995;40:245-67. doi:10.1146/annurev.en.40.010195.001333.
26. Tautz J, Maier S, Groh C, Rossler W, Brockmann A. Behavioral performance in adult honey bees is influenced by the temperature experienced during their pupal development. *Proc Natl Acad Sci U S A*. 2003;100(12):7343-7. doi:10.1073/pnas.1232346100.
27. Nagata T, Koyanagi M, Tsukamoto H, Terakita A. Identification and characterization of a

- 772 protostome homologue of peropsin from a jumping spider. *J Comp Physiol A Neuroethol Sens*
773 *Neural Behav Physiol.* 2010;196(1):51-9. doi:10.1007/s00359-009-0493-9.
- 774 28. Gulia-Nuss M, Nuss AB, Meyer JM, Sonenshine DE, Roe RM, Waterhouse RM et al. Genomic
775 insights into the *Ixodes scapularis* tick vector of Lyme disease. *Nat Commun.* 2016;7:10507.
776 doi:10.1038/ncomms10507.
- 777 29. Joseph RM, Carlson JR. *Drosophila* Chemoreceptors: A Molecular Interface Between the
778 Chemical World and the Brain. *Trends Genet.* 2015. doi:10.1016/j.tig.2015.09.005.
- 779 30. Croset V, Rytz R, Cummins SF, Budd A, Brawand D, Kaessmann H et al. Ancient protostome
780 origin of chemosensory ionotropic glutamate receptors and the evolution of insect taste and olfaction.
781 *PLoS Genet.* 2010;6(8):e1001064. doi:10.1371/journal.pgen.1001064.
- 782 31. Rytz R, Croset V, Benton R. Ionotropic receptors (IRs): chemosensory ionotropic glutamate
783 receptors in *Drosophila* and beyond. *Insect Biochem Mol Biol.* 2013;43(9):888-97.
784 doi:10.1016/j.ibmb.2013.02.007.
- 785 32. Chen C, Buhl E, Xu M, Croset V, Rees JS, Lilley KS et al. *Drosophila* Ionotropic Receptor 25a
786 mediates circadian clock resetting by temperature. *Nature.* 2015;527(7579):516-20.
787 doi:10.1038/nature16148.
- 788 33. Ni L, Klein M, Svec KV, Budelli G, Chang EC, Ferrer AJ et al. The Ionotropic Receptors IR21a
789 and IR25a mediate cool sensing in *Drosophila*. *Elife.* 2016;5. doi:10.7554/eLife.13254.
- 790 34. Cruz MDS, Robles MCV, Jespersen JB, Kilpinen O, Birkett M, Dewhurst S et al. Scanning
791 electron microscopy of foreleg tarsal sense organs of the poultry red mite, *Dermanyssus gallinae*
792 (DeGeer) (Acari : Dermanyssidae). *Micron.* 2005;36(5):415-21. doi:10.1016/j.micron.2005.03.003.
- 793 35. Robertson HM, Warr CG, Carlson JR. Molecular evolution of the insect chemoreceptor gene
794 superfamily in *Drosophila melanogaster*. *Proc Natl Acad Sci U S A.* 2003;100 Suppl 2:14537-42.
795 doi:10.1073/pnas.2335847100.
- 796 36. Chipman AD, Ferrier DE, Brena C, Qu J, Hughes DS, Schröder R et al. The first myriapod
797 genome sequence reveals conservative arthropod gene content and genome organisation in the
798 centipede *Strigamia maritima*. *PLoS Biol.* 2014;12(11):e1002005. doi:10.1371/journal.pbio.1002005.
- 799 37. Li X, Schuler MA, Berenbaum MR. Molecular mechanisms of metabolic resistance to synthetic
800 and natural xenobiotics. *Annu Rev Entomol.* 2007;52:231-53.
801 doi:10.1146/annurev.ento.51.110104.151104.
- 802 38. Iga M, Kataoka H. Recent studies on insect hormone metabolic pathways mediated by
803 cytochrome P450 enzymes. *Biol Pharm Bull.* 2012;35(6):838-43.
- 804 39. Toutant JP. Insect acetylcholinesterase: catalytic properties, tissue distribution and molecular
805 forms. *Prog Neurobiol.* 1989;32(5):423-46.
- 806 40. Dermauw W, Van Leeuwen T. The ABC gene family in arthropods: comparative genomics and
807 role in insecticide transport and resistance. *Insect Biochem Mol Biol.* 2014;45:89-110.
808 doi:10.1016/j.ibmb.2013.11.001.
- 809 41. Kirkness EF, Haas BJ, Sun W, Braig HR, Perotti MA, Clark JM et al. Genome sequences of the
810 human body louse and its primary endosymbiont provide insights into the permanent parasitic
811 lifestyle. *Proc Natl Acad Sci U S A.* 2010;107(27):12168-73. doi:10.1073/pnas.1003379107.
- 812 42. Wu K, Hoy MA. The Glutathione-S-Transferase, Cytochrome P450 and Carboxyl/Cholinesterase
813 Gene Superfamilies in Predatory Mite *Metaseiulus occidentalis*. *PLoS One.* 2016;11(7):e0160009.

- 814 doi:10.1371/journal.pone.0160009.
- 815 43. Enayati AA, Ranson H, Hemingway J. Insect glutathione transferases and insecticide resistance.
816 *Insect Mol Biol.* 2005;14(1):3-8. doi:10.1111/j.1365-2583.2004.00529.x.
- 817 44. Yu QY, Lu C, Li WL, Xiang ZH, Zhang Z. Annotation and expression of carboxylesterases in the
818 silkworm, *Bombyx mori*. *BMC Genomics.* 2009;10:553. doi:10.1186/1471-2164-10-553.
- 819 45. Gempe T, Beye M. Function and evolution of sex determination mechanisms, genes and
820 pathways in insects. *Bioessays.* 2011;33(1):52-60. doi:10.1002/bies.201000043.
- 821 46. Nelson-Rees WA, Hoy MA, Roush RT. Heterochromatinization, chromatin elimination and
822 haploidization in the parahaploid mite *Metaseiulus occidentalis* (Nesbitt) (Acarina: Phytoseiidae).
823 *Chromosoma.* 1980;77(3):263-76.
- 824 47. Sutovsky P. Sperm proteasome and fertilization. *Reproduction.* 2011;142(1):1-14.
825 doi:10.1530/REP-11-0041.
- 826 48. Baker ME. Evolution of 17beta-hydroxysteroid dehydrogenases and their role in androgen,
827 estrogen and retinoid action. *Mol Cell Endocrinol.* 2001;171(1-2):211-5.
- 828 49. Britton C, Murray L. Cathepsin L protease (CPL-1) is essential for yolk processing during
829 embryogenesis in *Caenorhabditis elegans*. *J Cell Sci.* 2004;117(Pt 21):5133-43.
830 doi:10.1242/jcs.01387.
- 831 50. Mediannikov O, Sekeyová Z, Birg ML, Raoult D. A novel obligate intracellular
832 gamma-proteobacterium associated with ixodid ticks, *Diplorickettsia massiliensis*, Gen. Nov., Sp.
833 Nov. *PLoS One.* 2010;5(7):e11478. doi:10.1371/journal.pone.0011478.
- 834 51. Chaisiri K, McGarry JW, Morand S, Makepeace BL. Symbiosis in an overlooked microcosm: a
835 systematic review of the bacterial flora of mites. *Parasitology.* 2015;142(9):1152-62.
836 doi:10.1017/S0031182015000530.
- 837 52. Dunning Hotopp JC, Clark ME, Oliveira DC, Foster JM, Fischer P, Muñoz Torres MC et al.
838 Widespread lateral gene transfer from intracellular bacteria to multicellular eukaryotes. *Science.*
839 2007;317(5845):1753-6. doi:10.1126/science.1142490.
- 840 53. Leclerque A. Whole genome-based assessment of the taxonomic position of the arthropod
841 pathogenic bacterium *Rickettsiella grylli*. *FEMS Microbiol Lett.* 2008;283(1):117-27.
842 doi:10.1111/j.1574-6968.2008.01158.x.
- 843 54. Yang B, Peng G, Li T, Kadowaki T. Molecular and phylogenetic characterization of honey bee
844 viruses, *Nosema* microsporidia, protozoan parasites, and parasitic mites in China. *Ecol Evol.*
845 2013;3(2):298-311. doi:10.1002/ece3.464.
- 846 55. Erban T, Harant K, Hubalek M, Vitamvas P, Kamler M, Poltronieri P et al. In-depth proteomic
847 analysis of *Varroa destructor*: Detection of DWV-complex, ABPV, VdMLV and honeybee proteins in
848 the mite. *Sci Rep.* 2015;5:13907. doi:10.1038/srep13907.
- 849 56. Mordecai GJ, Wilfert L, Martin SJ, Jones IM, Schroeder DC. Diversity in a honey bee pathogen:
850 first report of a third master variant of the Deformed Wing Virus quasispecies. *ISME J.*
851 2016;10(5):1264-73. doi:10.1038/ismej.2015.178.
- 852 57. Martin S, Highfield A, Brettell L, Villalobos E, Budge G, Powell M et al. Global Honey Bee Viral
853 Landscape Altered by a Parasitic Mite. *Science.* 2012;336(6086):1304-6.
854 doi:10.1126/science.1220941.
- 855 58. Anderson DL, Morgan MJ. Genetic and morphological variation of bee-parasitic *Tropilaelaps*

- 856 mites (Acari: Laelapidae): new and re-defined species. *Exp Appl Acarol.* 2007;43(1):1-24.
857 doi:10.1007/s10493-007-9103-0.
- 858 59. Martin M. Cutadapt removes adapter sequences from highthroughput sequencing reads. *EMBnet.*
859 *journal* 17: 10–12. 2011.
- 860 60. Joshi N, Fass J. Sickle: A sliding-window, adaptive, quality-based trimming tool for FastQ files
861 (Version 1.33)[Software]. Available at <https://github.com/najoshi/sickle>. 2011.
- 862 61. Adams MD, Celniker SE, Holt RA, Evans CA, Gocayne JD, Amanatides PG et al. The genome
863 sequence of *Drosophila melanogaster*. *Science.* 2000; 287(5461):2185-95.
864 doi:10.1126/science.287.5461.2185
- 865 62. Weinstock G, Robinson G, Gibbs R, Worley K, Evans J, Maleszka R et al. Insights into social
866 insects from the genome of the honeybee *Apis mellifera*. *Nature.* 2006;443(7114):931-49.
867 doi:10.1038/nature05260.
- 868 63. Marcais G, Kingsford C. A fast, lock-free approach for efficient parallel counting of occurrences
869 of k-mers. *Bioinformatics.* 2011;27(6):764-70. doi:10.1093/bioinformatics/btr011.
- 870 64. Zhang G, Fang X, Guo X, Li L, Luo R, Xu F et al. The oyster genome reveals stress adaptation
871 and complexity of shell formation. *Nature.* 2012;490(7418):49-54. doi:10.1038/nature11413.
- 872 65. Langmead B, Salzberg SL. Fast gapped-read alignment with Bowtie 2. *Nature Methods.*
873 2012;9(4):357-9.
- 874 66. Zerbino D, Birney E. Velvet: Algorithms for de novo short read assembly using de Bruijn graphs.
875 *Genome Res.* 2008;18(5):821-9. doi:10.1101/gr.074492.107.
- 876 67. Kumar S, Jones M, Koutsovoulos G, Clarke M, Blaxter M. Blobology: exploring raw genome
877 data for contaminants, symbionts and parasites using taxon-annotated GC-coverage plots. *Front*
878 *Genet.* 2013;4:237.
- 879 68. Benson G. Tandem repeats finder: a program to analyze DNA sequences. *Nucleic Acids Res.*
880 1999;27(2):573-80. doi:10.1093/nar/27.2.573.
- 881 69. Trapnell C, Pachter L, Salzberg S. TopHat: discovering splice junctions with RNA-Seq.
882 *Bioinformatics.* 2009;25(9):1105-11. doi:10.1093/bioinformatics/btp120.
- 883 70. Trapnell C, Williams BA, Pertea G, Mortazavi A, Kwan G, van Baren MJ et al. Transcript
884 assembly and quantification by RNA-Seq reveals unannotated transcripts and isoform switching
885 during cell differentiation. *Nat Biotechnol.* 2010;28(5):511-5. doi:10.1038/nbt.1621.
- 886 71. Liu J, Xiao H, Huang S, Li F. OMIGA: optimized maker-based insect genome annotation. *Mol*
887 *Genet Genomics.* 2014;289(4):567-73.
- 888 72. Stanke M, Morgenstern B. AUGUSTUS: a web server for gene prediction in eukaryotes that
889 allows user-defined constraints. *Nucleic Acids Res.* 2005;33:W465-W7. doi:10.1093/nar/gki458.
- 890 73. Korf I. Gene finding in novel genomes. *BMC Bioinformatics.* 2004;5.
891 doi:10.1186/1471-2105-5-59.
- 892 74. Lukashin AV, Borodovsky M. GeneMark.hmm: new solutions for gene finding. *Nucleic Acids*
893 *Res.* 1998;26(4):1107-15.
- 894 75. Cantarel B, Korf I, Robb S, Parra G, Ross E, Moore B et al. MAKER: An easy-to-use annotation
895 pipeline designed for emerging model organism genomes. *Genome Res.* 2008;18(1):188-96.
896 doi:10.1101/gr.6743907.
- 897 76. Zdobnov EM, Apweiler R. InterProScan--an integration platform for the signature-recognition

898 methods in InterPro. *Bioinformatics*. 2001;17(9):847-8.

899 77. Lowe TM, Eddy SR. tRNAscan-SE: a program for improved detection of transfer RNA genes in
900 genomic sequence. *Nucleic Acids Res*. 1997;25(5):955-64.

901 78. Nawrocki EP, Eddy SR. Infernal 1.1: 100-fold faster RNA homology searches. *Bioinformatics*.
902 2013;29(22):2933-5. doi:10.1093/bioinformatics/btt509.

903 79. Conesa A, Götz S, García-Gómez JM, Terol J, Talón M, Robles M. Blast2GO: a universal tool
904 for annotation, visualization and analysis in functional genomics research. *Bioinformatics*.
905 2005;21(18):3674-6. doi:10.1093/bioinformatics/bti610.

906 80. Kanehisa M, Goto S. KEGG: kyoto encyclopedia of genes and genomes. *Nucleic Acids Res*.
907 2000;28(1):27-30.

908 81. Katoh K, Standley DM. MAFFT multiple sequence alignment software version 7: improvements
909 in performance and usability. *Mol Biol Evol*. 2013;30(4):772-80. doi:10.1093/molbev/mst010.

910 82. Lassmann T, Frings O, Sonnhammer EL. Kalign2: high-performance multiple alignment of
911 protein and nucleotide sequences allowing external features. *Nucleic Acids Res*. 2009;37(3):858-65.
912 doi:10.1093/nar/gkn1006.

913 83. Castresana J. Selection of conserved blocks from multiple alignments for their use in
914 phylogenetic analysis. *Mol Biol Evol*. 2000;17(4):540-52.

915 84. Darriba D, Taboada GL, Doallo R, Posada D. ProtTest 3: fast selection of best-fit models of
916 protein evolution. *Bioinformatics*. 2011;27(8):1164-5. doi:10.1093/bioinformatics/btr088.

917 85. Guindon S, Dufayard JF, Lefort V, Anisimova M, Hordijk W, Gascuel O. New algorithms and
918 methods to estimate maximum-likelihood phylogenies: assessing the performance of PhyML 3.0.
919 *Syst Biol*. 2010;59(3):307-21. doi:10.1093/sysbio/syq010.

920 86. Ronquist F, Huelsenbeck JP. MrBayes 3: Bayesian phylogenetic inference under mixed models.
921 *Bioinformatics*. 2003;19(12):1572-4.

922 87. Tamura K, Stecher G, Peterson D, Filipowski A, Kumar S. MEGA6: Molecular Evolutionary
923 Genetics Analysis version 6.0. *Mol Biol Evol*. 2013;30(12):2725-9. doi:10.1093/molbev/mst197.

924 88. Adams M, Celniker S, Holt R, Evans C, Gocayne J, Amanatides P et al. The genome sequence of
925 *Drosophila melanogaster*. *Science*. 2000;287(5461):2185-95. doi:10.1126/science.287.5461.2185.

926 89. Sanggaard KW, Bechsgaard JS, Fang X, Duan J, Dyrland TF, Gupta V et al. Spider genomes
927 provide insight into composition and evolution of venom and silk. *Nat Commun*. 2014;5:3765.
928 doi:10.1038/ncomms4765.

929 90. Stein L, Sternberg P, Durbin R, Thierry-Mieg J, Spieth J. WormBase: network access to the
930 genome and biology of *Caenorhabditis elegans*. *Nucleic Acids Res*. 2001;29(1):82-6.
931 doi:10.1093/nar/29.1.82.

932 91. Dabert M, Witalinski W, Kazmierski A, Olszanowski Z, Dabert J. Molecular phylogeny of
933 acariform mites (Acari, Arachnida): strong conflict between phylogenetic signal and long-branch
934 attraction artifacts. *Mol Phylogenet Evol*. 2010;56(1):222-41. doi:10.1016/j.ympev.2009.12.020.

935 92. Yang Z. PAML 4: phylogenetic analysis by maximum likelihood. *Mol Biol Evol*.
936 2007;24(8):1586-91. doi:10.1093/molbev/msm088.

937 93. Li L, Stoeckert CJ, Roos DS. OrthoMCL: identification of ortholog groups for eukaryotic
938 genomes. *Genome Res*. 2003;13(9):2178-89. doi:10.1101/gr.1224503.

939 94. De Bie T, Cristianini N, Demuth JP, Hahn MW. CAFE: a computational tool for the study of gene

940 family evolution. *Bioinformatics*. 2006;22(10):1269-71. doi:10.1093/bioinformatics/btl097.

941 95. Grabherr MG, Haas BJ, Yassour M, Levin JZ, Thompson DA, Amit I et al. Full-length
942 transcriptome assembly from RNA-Seq data without a reference genome. *Nature Biotech.*
943 2011;29(7):644-52.

944 96. Li B, Dewey CN. RSEM: accurate transcript quantification from RNA-Seq data with or without
945 a reference genome. *BMC bioinformatics*. 2011;12(1):1.

946 97. Anders S, Pyl PT, Huber W. HTSeq--a Python framework to work with high-throughput
947 sequencing data. *Bioinformatics*. 2015;31(2):166-9. doi:10.1093/bioinformatics/btu638.

948 98. Robinson MD, McCarthy DJ, Smyth GK. edgeR: a Bioconductor package for differential
949 expression analysis of digital gene expression data. *Bioinformatics*. 2010;26(1):139-40.
950 doi:10.1093/bioinformatics/btp616.

951 99. Bourgon R, Gentleman R, Huber W. Independent filtering increases detection power for
952 high-throughput experiments. *Proc Natl Acad Sci U S A*. 2010;107(21):9546-51.
953 doi:10.1073/pnas.0914005107.

954 100. Dimont E, Shi J, Kirchner R, Hide W. edgeRun: an R package for sensitive, functionally
955 relevant differential expression discovery using an unconditional exact test. *Bioinformatics*.
956 2015;31(15):2589-90. doi:10.1093/bioinformatics/btv209.

957 101. Elsik CG, Worley KC, Bennett AK, Beye M, Camara F, Childers CP et al. Finding the missing
958 honey bee genes: lessons learned from a genome upgrade. *BMC Genomics*. 2014;15:86.
959 doi:10.1186/1471-2164-15-86.

960 102. Vizcaíno JA, Csordas A, del-Toro N, Dianes JA, Griss J, Lavidas I et al. 2016 update of the
961 PRIDE database and its related tools. *Nucleic Acids Res*. 2016;44(D1):D447-56.
962 doi:10.1093/nar/gkv1145.

963 103. Mounsey KE, Willis C, Burgess ST, Holt DC, McCarthy J, Fischer K. Quantitative PCR-based
964 genome size estimation of the astigmatid mites *Sarcoptes scabiei*, *Psoroptes ovis* and
965 *Dermatophagoides pteronyssinus*. *Parasit Vectors*. 2012;5(1):1.

966 104. Sánchez - Gracia A, Vieira FG, Almeida FC, Rozas J. Comparative genomics of the major
967 chemosensory gene families in Arthropods. *eLS*. 2011.

968 105. Feyereisen R, Lawrence I. 8–insect CYP genes and P450 enzymes. *Insect Mol Bio Biochem*.
969 2012:236-316.

972 Table 1 Genome statistics of *T. mercedesae* and other arachnid species

Species	Acari: Parasitiformes				Acari: Acariformes			Araneae		Scorpiones
	<i>Tropilaelaps mercedesae</i>	<i>Metaseiulus occidentalis</i>	<i>Varroa destructor</i>	<i>Ixodes scapularis</i>	<i>Dermatophagoides farinae</i>	<i>Sarcoptes scabiei</i>	<i>Tetranychus urticae</i>	<i>Stegodyphus mimosarum</i>	<i>Acanthoscurria geniculata</i>	<i>Mesobuthus martensii</i>
Estimated genome size (Mb)	660	88-90	565	2,100	-	98	90	2,550	6,500	1,323
Assembled genome Size (Mb)	353	152	294	1,765	54	56	91	2,739	7,178	926
GC content (%)	44	52	41	45	30	38	32	34	39	30
Total scaffold number	34,155	2,211	na	369,492	515	18,860	640	68,653	4,986,575	na
Largest scaffold (kb)	327,111	2,438,724	na	3,698,136	771,048	287,415	6,836,010	2,994,948	819,799	340,307
N50 size (bp)	28,807	896,831	na	76,228	186,342	na	2,993,488	480,636	47,837	223,560
Complete CEGs (%)	92	98	68	80	98	98	98	62	33	57
Partial CEGs (%)	98	97	32	42	96	94	95	24	15	24
Number of protein-coding genes	15,190	18,338 11,430	11,432	20,486	16,376	10,473 10,644	18,414 18,224	27,135	27,235	73,821
Average exon length (bp)	363	262	na	187	na	347	334	174	na	na
Average intron length (bp)	820	647	na	2,653	na	147	477	4,269	na	na

973 Data referred to this study and [11, 15, 16, 28, 89, 103].

974
975
976 Table 2 The number of genes associated with chemosensory system in *T. mercedesae* and other arthropods.

Species	GR	OR	IR	OBP	CSP
<i>T. mercedesae</i>	5	0	8	0	0
<i>M. occidentalis</i>	64	0	65	0	0
<i>I. scapularis</i>	60	0	22	0	1
<i>S. maritima</i>	77	0	60	0	2
<i>D. pulex</i>	53	0	85	0	3
<i>D. melanogaster</i>	73	62	66	51	4
<i>A. mellifera</i>	10	163	10	21	6
<i>B. mori</i>	56	48	18	44	18
<i>A. pisum</i>	53	48	11	15	13
<i>P. humanus</i>	8	10	12	5	7

977
978 The numbers of GR (gustatory receptor), OR (olfactory receptor), IR (ionotropic receptor), OBP (olfactory binding protein), and CSP (chemosensory protein) genes in *T. mercedesae* and nine arthropod species including *Bombyx mori* and *Acyrtosiphon pisum* are shown. Data referred to references [36, 104, 21] and this study.

983 Table 3 Comparison of the number of CYP2, 3, 4, and mitochondrial clan members in Insecta,
 984 Crustacea, and Acari.

	Total	CYP2	CYP3	CYP4	Mitochondria
Insecta					
<i>D. melanogaster</i>	88	7	11	32	36
<i>A. gambiae</i>	105	10	9	46	40
<i>A. aegypti</i>	160	12	9	57	82
<i>B. mori</i>	85	7	12	36	30
<i>A. mellifera</i>	46	8	6	4	28
<i>N. vitripennis</i>	92	7	7	30	48
<i>T. castaneum</i>	134	8	9	45	72
<i>A. pisum</i>	64	10	8	23	23
<i>P. humanus</i>	36	8	8	9	11
Crustacea					
<i>D. pulex</i>	75	20	6	37	12
Acari					
<i>T. mercedesae</i>	56	7	19	20	10
<i>M. occidentalis</i>	75 (63)	19 (16)	32 (23)	19	5
<i>T. urticae</i>	86	48	5	23	10

985 The data of four insects, *Anopheles gambiae*, *Aedes aegypti*, *Nasonia vitripennis*, and *Tribolium*
 986 *castaneum* are also included. Data referred to references [105] and this study. The numbers in
 987 parentheses are derived from previous report [42].

989 **Figure legends**

990 **Figure 1 Images of *Tropilaelaps mercedesae***

991 (A) Three adult females of *T. mercedesae* infesting the 5th instar honey bee larva. (B) Ventral view
992 of the nymph (immature female). (C) Ventral view of the adult female.

994 **Figure 2 Comparative genomics.**

995 (A) The species phylogeny was built from aligned protein sequences of 926 one-to-one orthologs in
996 *Metaseiulus occidentalis*, *Tropilaelaps mercedesae*, *Ixodes scapularis*, *Stegodyphus mimosarum*,
997 *Tetranychus urticae*, *Drosophila melanogaster*, *Apis mellifera* and *Caenorhabditis elegans* using a
998 maximum likelihood method. The tree was rooted with *C. elegans*. All nodes showed 100%
999 bootstrap support. Protein-coding genes were classified into the different categories. 1:1:1 orthologs
1000 and N:N:N orthologs represent the common orthologs with the same copy numbers and different
1001 copy numbers, respectively. Patchy orthologs are shared between more than one but not all species
1002 (excluding those in the previous categories). Unclustered genes represent genes which were not
1003 classified into orthology cluster. Other categories include arthropod-, Arachnida-, Parasitiformes-,
1004 and species-specific genes. *C. elegans* was used as the outgroup for classification of the
1005 protein-coding genes. (B) The number of gene families shared between *T. mercedesae*, *M.*
1006 *occidentalis*, *I. scapularis*, and other reference species (*S. mimosarum*, *T. urticae*, *D. melanogaster*,
1007 *A. mellifera* and *C. elegans*) by orthoMCL classification algorithm.

1008
1009 **Figure 3 Phylogenetic tree of *T. mercedesae*, *I. scapularis*, and *D. melanogaster* gustatory receptors.**

1010 Phylogenetic tree of *T. mercedesae* (red), *I. scapularis* (blue), and *D. melanogaster* (green) gustatory
1011 receptors (GRs) was constructed by a maximum likelihood method. Two clusters of fruit fly GRs
1012 responding to sugar and CO₂ are indicated. The tree was rooted at the middle point.

1014
1015 **Figure 4 Phylogeny of *T. mercedesae*, *M. occidentalis*, and *D. melanogaster* cytochrome P450.**

1016 The phylogenetic tree was constructed by maximum likelihood method and rooted at the middle
1017 point. P450s are clustered to CYP2, CYP3, CYP4, and mitochondrial clans are shown by red, green,
1018 blue, and dark yellow branches, respectively. *D. melanogaster* (DmCYP), *T. mercedesae*, and *M.*
1019 *occidentalis* P450s are indicated by dark green, purple, and dark yellow, respectively. *T. mercedesae*
1020 and *M. occidentalis* P450s are designated by protein IDs.

1021
1022 **Figure 5 Volcano plot of proteins in the male and female mites.**

1023 Proteins identified in the male and female mites by proteomic analysis are plotted according to the
1024 ratios of amounts present in male to female. Proteins abundant in the male and female are indicated
1025 by blue and red circles, respectively. Some of the representative proteins are indicated with the
1026 names and accession numbers of the best Blast hits.

1027
1028 **Figure 6 %GC-coverage plots of the preliminary assembled genomes of male and female.**

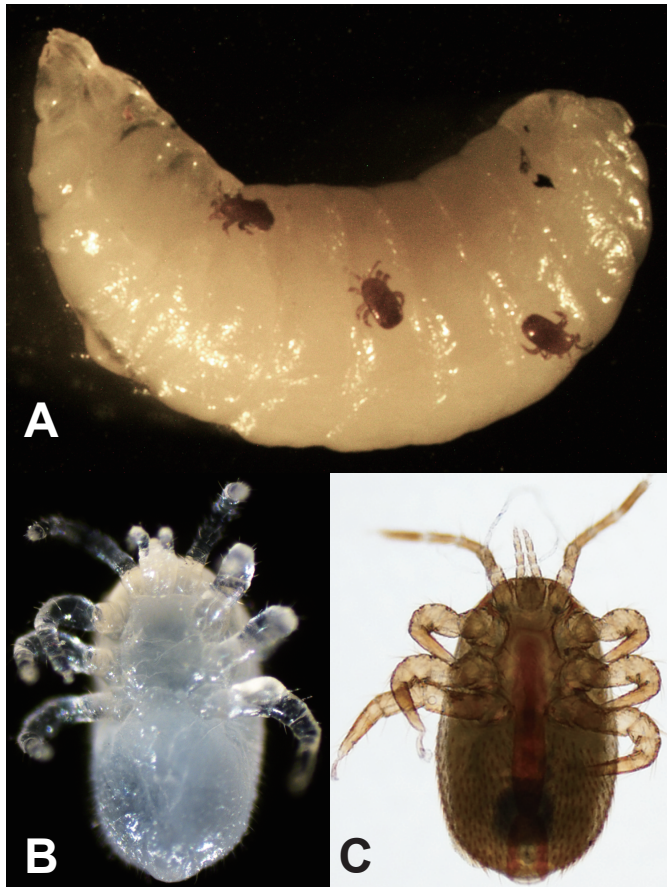
1029 Individual contigs are plotted based on their GC content (x-axis) and their node coverage (y-axis;
1030 logarithmic scale). Contigs are colored according to the taxonomic order of their best Megablast hit

1031 to the NCBI nt database (with E-value cut off $< 1e-5$). Contigs without the annotation are in gray. %
1032 GC plots against node coverage for the (A) male and (B) female contigs are shown in.

1033
1034 **Figure 7 Classification of DWV in the *T. mercedesae* transcriptomes.**

1035 The Bayesian phylogeny was constructed using Mrbayes based on the amino acid sequences of
1036 complete DWV genomes assembled from the adult males, adult females and nymphs transcriptomes
1037 (DWV weixi strain complete genome male, DWV weixi strain complete genome female, and DWV
1038 weixi strain complete genome nymph) as well as seven other DWV strains (type A variant:
1039 NC_005876.1, NC_004830.2, JQ_413340, and ERS657948; type B: KC_786222.1 and
1040 NC_006494.1; type C: ERS657949). The tree was rooted with Formica exsecta Virus 1
1041 (NC_023022.1) and Sacbrood Virus (NC_002066.1).

1042
17
18
19
20
21
22
23
24
25
26
27
28
29
30
31
32
33
34
35
36
37
38
39
40
41
42
43
44
45
46
47
48
49
50
51
52
53
54
55
56
57
58
59
60
61
62
63
64
65



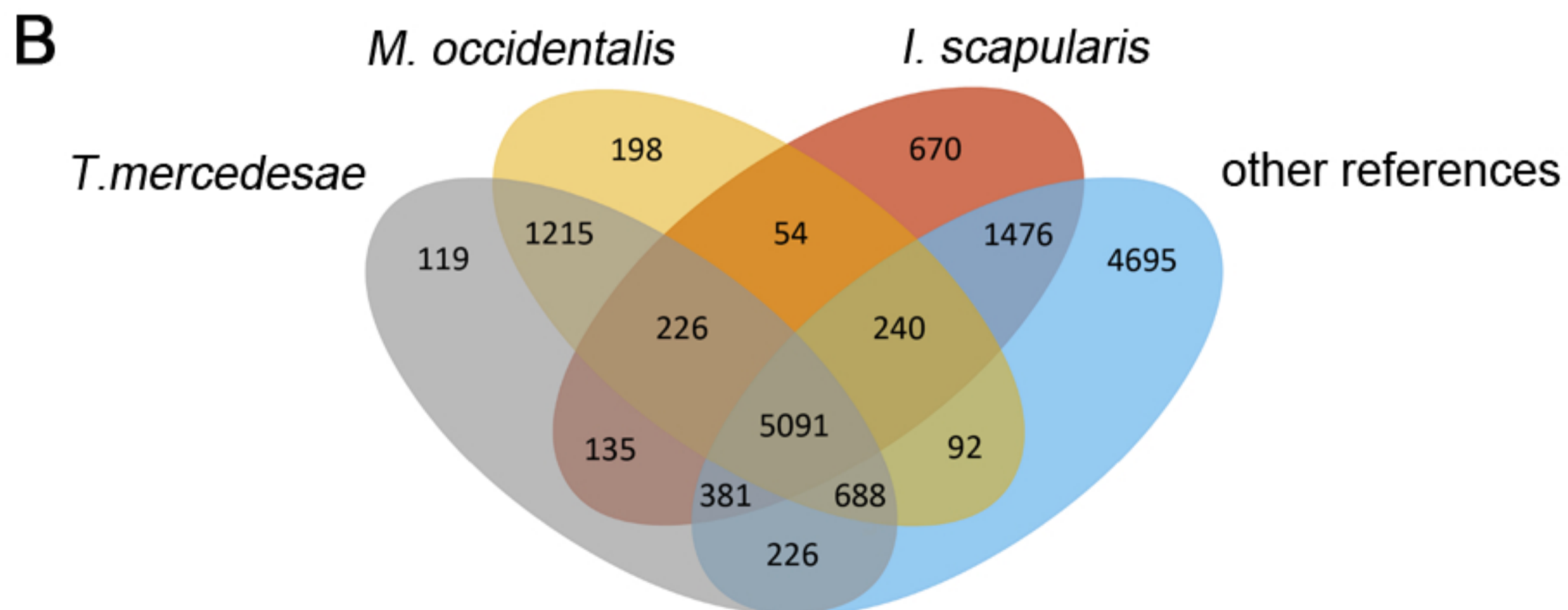
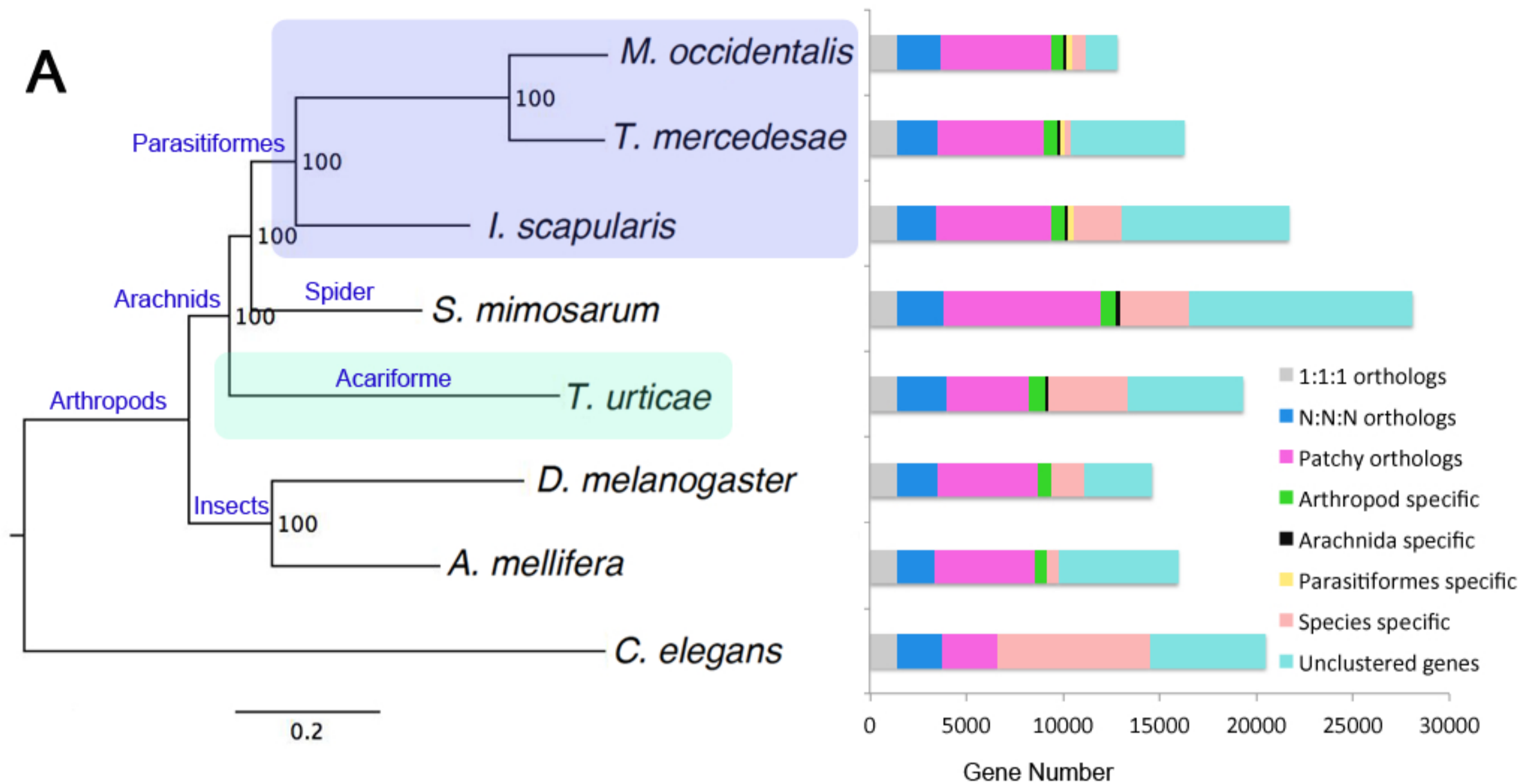
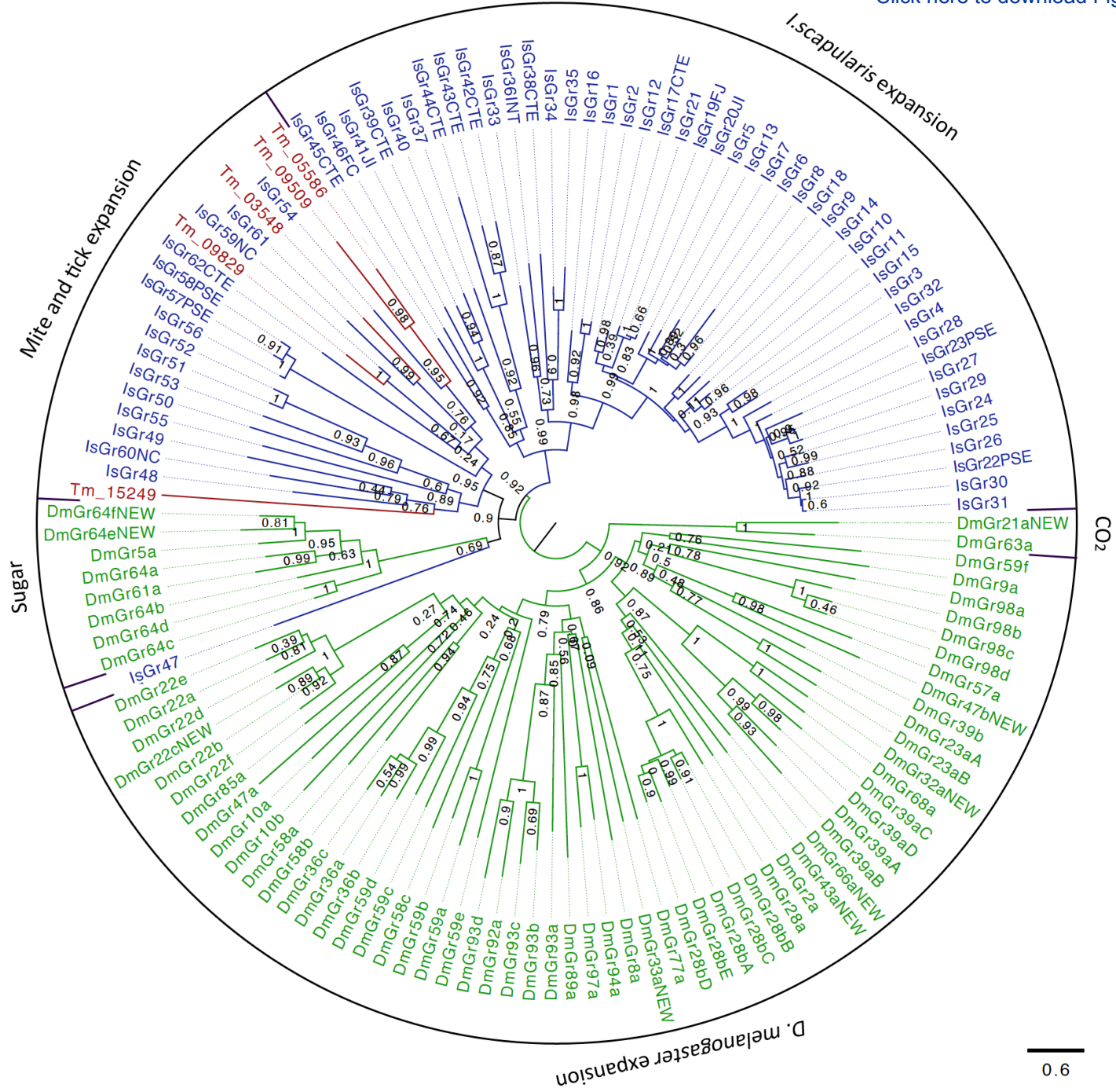
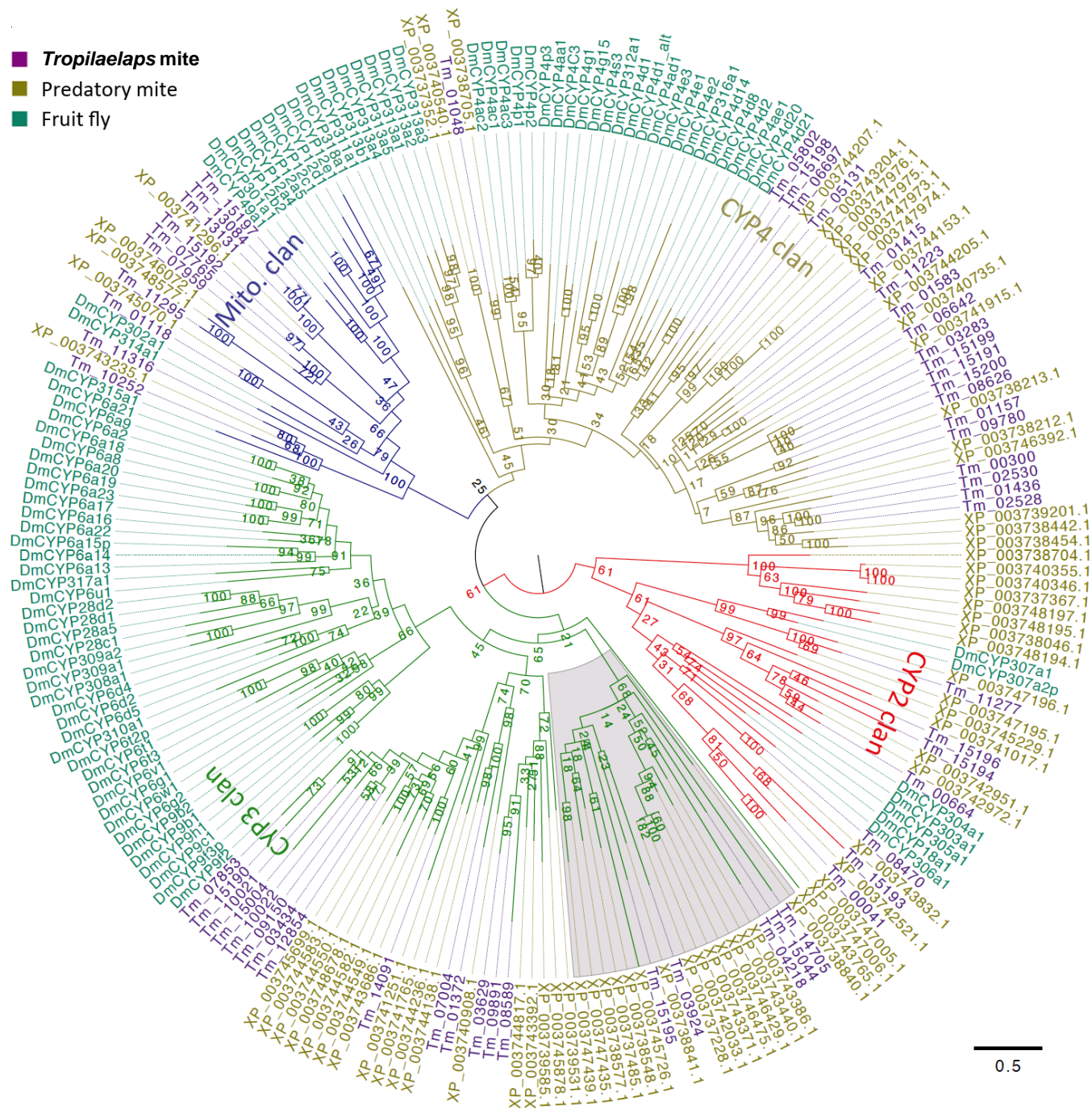


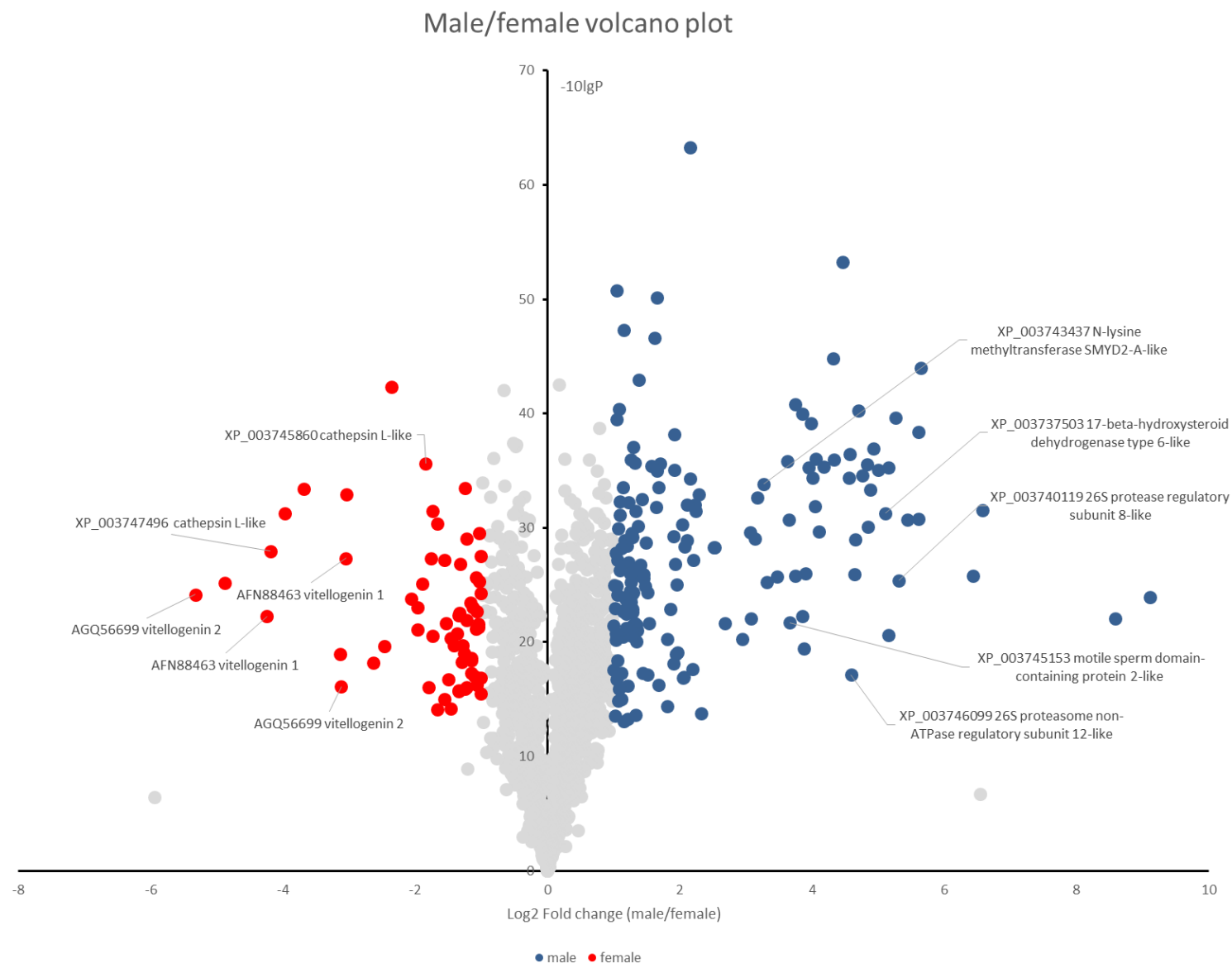
Figure 3

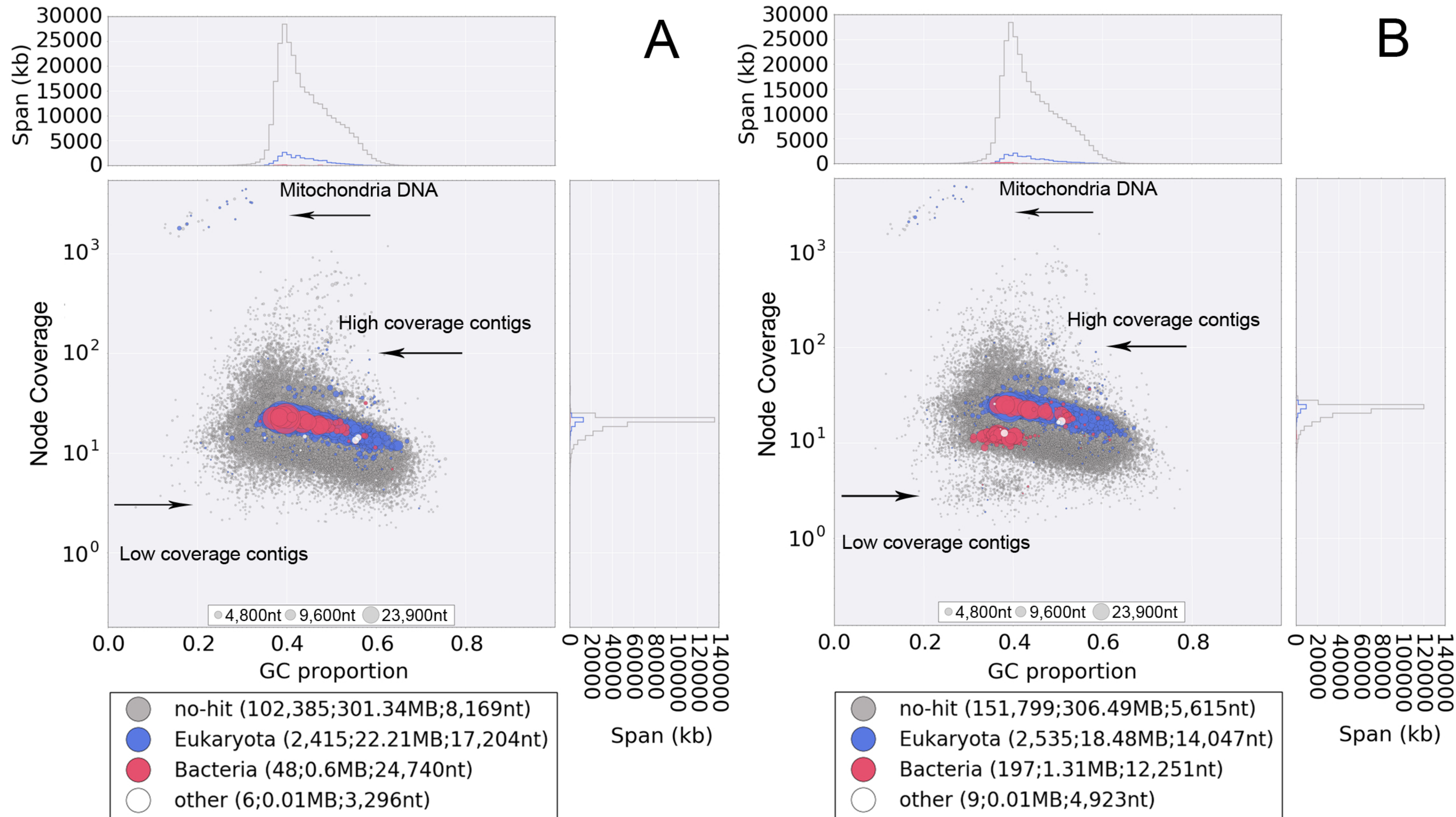


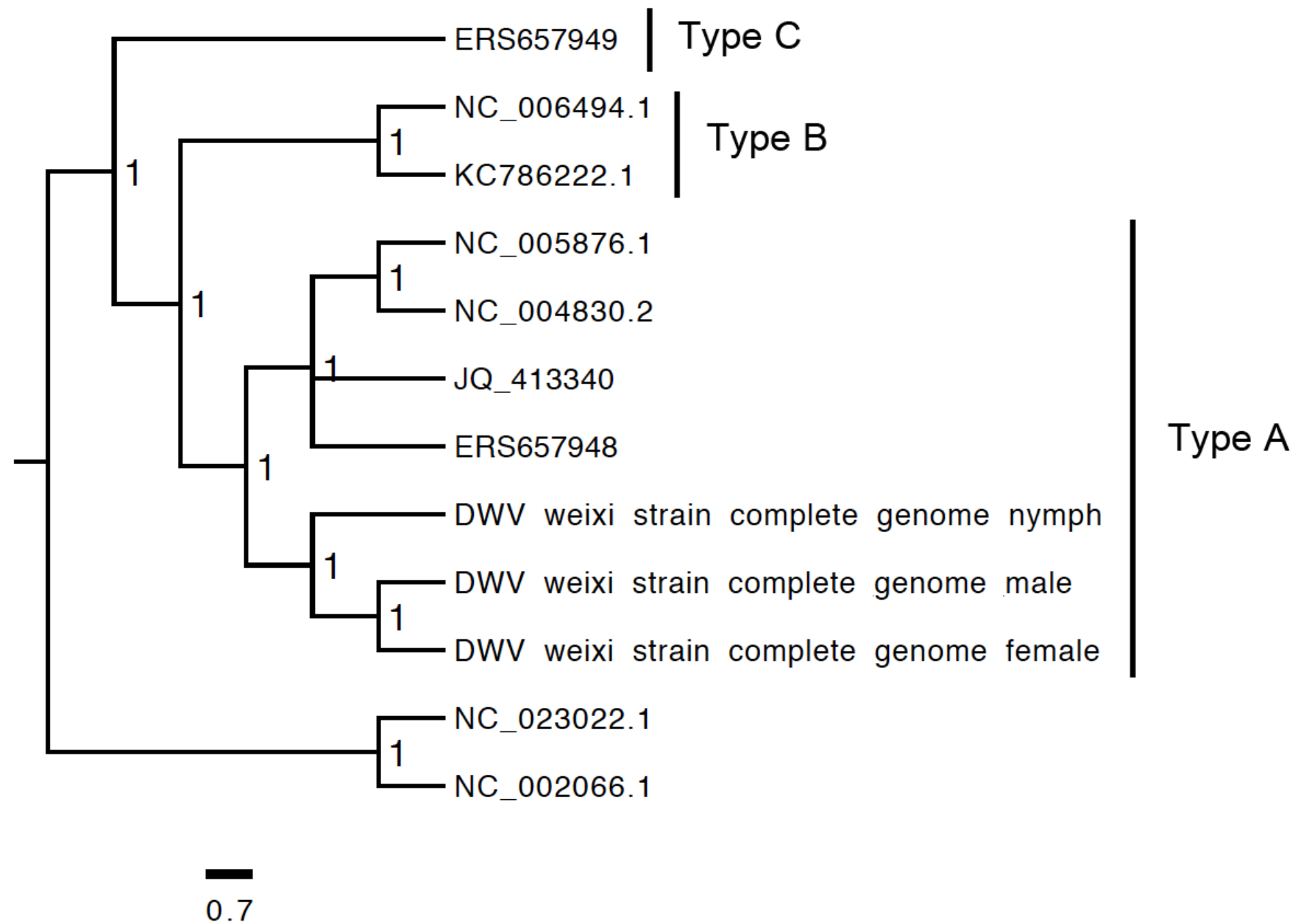
0.6

- *Tropilaelaps* mite
- Predatory mite
- Fruit fly













Click here to access/download
Supplementary Material
Dong et al_Supplementary Figures.doc





Click here to access/download
Supplementary Material
Dong et al_Supplementary Tables.doc

